

**STUDIES OF EARTH DYNAMICS WITH
THE SUPERCONDUCTING GRAVIMETER**

Heikki Virtanen

HELSINKI 2006

**STUDIES OF EARTH DYNAMICS WITH
THE SUPERCONDUCTING GRAVIMETER**

Heikki Virtanen

Academic dissertation in Geophysics

To be presented, with the permission of the Faculty of Science
of the University of Helsinki, for public criticism in Physicum
Auditorium E204, on April 21, 2006, at 12 o'clock noon.

HELSINKI 2006

Also published as No. 133 in the series of

Suomen Geodeettisen laitoksen julkaisuja
Veröffentlichungen des Finnischen Geodätischen Institutes
Publications of the Finnish Geodetic Institute

ISBN-13: 958-951-711-255-0 (nid.)

ISBN-10: 951-711-255-6 (nid.)

ISBN-13: 978-952-10-3057-4 (PDF)

ISBN-10: 952-10-3057-7 (PDF)

“...Concluding on a lighter topic, let me remind the GGP community of what I recall as probably the most memorable moment of the first campaign. It occurred at the GGP Workshop in Munsbach Castle, 1999, when Virtanen was describing the effect of snow cover on the residual gravity at Metsahovi. He showed a figure of gravity increasing by about 2 microgal over a 4-h period as men shoveled snow from the roof of the SG station, when a member of the audience asked why there was an interruption in the rise of gravity, Heikki said this was a 'tea break'...”

D. Crossley, in *Journal of Geodynamics* 38/3-4 (2004), p. 234.

Abstract

I present investigations of Earth dynamics with the superconducting gravimeter GWR T020 at Metsähovi from 1994 to 2005. As a necessary background, the history and key technical details of the installation are given. Then a new data acquisition system (DAS) developed by the author is described. It has proved reliable and accurate. A pre-requisite for the study of weak phenomena is the removal of the tides from the gravity record and the careful treatment of spikes, offsets and drifts. I present the data processing methods and the development of the local tidal model at Metsähovi and show that improvements help in the modelling of long-term environmental effects.

First, I have used the T020 as a long-period seismometer to study microseismicity and the Earth's free oscillation. I present the annual variation, spectral distribution, amplitude and the sources of microseism at Metsähovi. High levels of microseism appear to be mainly generated by low-pressure areas (storms) in the Northern Atlantic.

I have analyzed free oscillations excited by three large earthquakes: the spectra, attenuation and rotational splitting of the modes. An air pressure correction is required to bring down the noise level. The lowest modes of all different oscillation types are studied, i.e. the radial mode ${}_0S_0$, the "football mode" ${}_0S_2$, and the toroidal mode ${}_0T_2$. This last-mentioned mode is very weak in the vertical as the component is only generated through the Coriolis coupling. I have also detected the very low level (0.01 nms^{-1}) incessant excitation of the Earth's free oscillation with the T020.

The recovery of global and regional variations in gravity with the superconducting gravimeter requires the modelling of local gravity effects. The most important of them is hydrology. The variation in the groundwater level at Metsähovi as measured in a borehole in the fractured bedrock correlates significantly (0.79) with gravity. The range of the gravity effect is 70 nms^{-2} and this phenomenon must be taken into account at an early stage of data processing. The influence of local precipitation, soil moisture and snow cover are detectable in the gravity record. A fortuitous experiment powerfully demonstrated the effect of snow on the laboratory roof, on that occasion -20 nms^{-2} .

The gravity effect of the variation in atmospheric mass (range about 300 nms^{-2}) and that of the non-tidal loading by the Baltic Sea (range about 50 nms^{-2}) were investigated together, as sea level and air pressure are correlated. The effects were modelled both using regression on the local barometer and tide gauge, and with a Green's function formalism based a detailed model of the load. In the regression approach, there is a trade-off between the coefficients. Using Green's functions it was calculated that a 1 metre uniform layer of water in the Baltic Sea increases the gravity at Metsähovi by 31 nms^{-2} and the vertical deformation is -11 mm . Best results were obtained using the HIRLAM (High Resolution Limited Area Model) for the atmosphere. Regression on the sea level in Helsinki then decreases the RMS of gravity residuals by 16%, i.e. explains about 30% of their variance. The regression coefficient for sea level is $27 \text{ nms}^{-2} \text{ m}^{-1}$, which is 87% of the uniform model. These studies are associated with temporal height variations using the GPS data of Metsähovi permanent station. Loading by air pressure and the Baltic Sea explains about 40% of the variance of daily GPS height solution.

Acknowledgements

I am grateful to the late Professor *Aimo Kiviniemi*, my former Department Chief and to Professor emeritus *Juhani Kakkuri*, retired Director General, who initiated the operational work with the superconducting gravimeter at Metsähovi.

The atmosphere at the Finnish Geodetic Institute has been favourable and encouraging for a research work. I would like to express my appreciation to Professor *Risto Kuittinen*, Director General, to Professor *Jussi Kääriäinen*, the former Chief of the Department of Gravimetry and to Professor *Markku Poutanen*, Chief of the Department of Geodesy and Geodynamics.

Special thanks to my mentor Doc. *Jaakko Mäkinen* for excellent advisement and for encouraging a scientific way of thinking for years.

I wish to express my gratitude for the fruitful co-operation with the Finnish Institute of Marine Research and the Finnish Meteorological Institute.

I wish to thank particularly my colleagues in the Department of Geodesy and Geodynamics for an assistance of maintenance the instrument and thanks are extended to the whole friendly staff of the institute.

My warmest thanks finally, got to my wife *Marjatta* and to my children *Riikka*, *Mikko* and *Venla* for their patience due to lengthy workdays throughout last years.

Helsinki, March 10, 2006

Heikki Virtanen

Contents

List of used abbreviations.....	8
List of publications.....	9
1. Introduction.....	10
1.1. Superconducting gravimeter as a research tool.....	10
1.2. Temporal variation in gravity.....	10
2. Installation and data processing.....	11
2.1. Site description.....	11
2.2. Operating history.....	13
2.3. Calibration.....	13
2.4. Data processing.....	13
2.5. The new data acquisition system.....	15
3. The seismic frequency band.....	18
3.1. Seismic background noise.....	18
3.2. Microseism.....	19
3.3. Free oscillation of the Earth.....	19
3.4. Incessant excitation of the Earth's free oscillation.....	21
4. The tidal frequency band.....	23
4.1. Tidal models at Metsähovi.....	23
4.2. Long period tides.....	25
5. Atmospheric effects and the Baltic Sea loading.....	26
5.1. Single admittance for air pressure and modeled Baltic Sea.....	26
5.2. Air pressure grid and single tide gauge.....	27
5.3. Vertical motion due to loading and GPS.....	27
5.4. The effects of different tidal models.....	27
6. Hydrological effects on gravity.....	28
6.1. Instrumentation and available data.....	28
6.2. Results of local studies.....	29
6.3. Regional and global hydrology.....	30
7. Summary and conclusions.....	31
References.....	32
Appendices 1,2,3.....	37
Publications I, II, III, IV, V and VI.....	43

List of used abbreviations

AP	air pressure
CHAMP	CHAllenging Minisatellite Payload
CSGI	Canadian Superconducting Gravimeter Installation
DAS	data acquisition system
DSL	Sea level at Degerby tidegauge
ETERNA	Eterna program package v. 3.30 (3.40), Wenzel, H-G, 1996)
FGI	Finnish Geodetic Institute
FCN	Free core nutation
GFZ	Geforschung Zentrum in Potsdam.
GGP	Global Geodynamics Project
GGP-ISDC	GGP Information System and Data Center (GFZ) (http://ggp.gfz-potsdam.de).
GGP1	Gravity card and filter in GGP project since 1997
GPS	Global Positioning System
GRACE	Gravity Recovery and Climate Experiment
GW	Groundwater level (local at Metsähovi)
GWR	Manufacturer of SG:s (San Diego, California, USA)
HIRLAM	High Resolution Limited Area Model (air pressure)
HSL	Sea level at Helsinki tidegauge
ICET	International Center for Earth Tides
LTM	Local tidal model
ME	Metsähovi station
MS	microseims
SG	superconducting gravimeter
SNM	Seismic Noise Magnitude
TSIP	Trimble Standard Interface Protocol
TSOFT	Software package for the analysis of time series and Earth tides
T020	SG at Metsähovi
WSFS	Watershed Simulation and Forecasting System

List of Publications

This thesis consists of 6 published papers and this review. The papers are referred using roman numerals in brackets. They are:

- I. Virtanen, H., 1996. Observations of free oscillations of the Earth by superconducting gravimeter GWR T020. *Acta Geod. Geoph. Mont. Hung.* Vol 31, 423-431.
- II. Virtanen, H., 1998. On superconducting gravimeter observations above 8 mHz at the Metsähovi station, Finland. *Rep. Finn. Geod. Inst.* 98:5.
- III. Virtanen H., 2000. On the observed hydrological environmental effects on gravity at the Metsähovi station, Finland. In B. Ducarme and J. Barthélemy (eds): Proceedings of the Workshop: High Precision Gravity Measurements with Application to Geodynamics, and Second GGP Workshop. Munsbach Castle (Grand Duchy of Luxembourg), March 24th to 26th. *Cahiers du Centre Européen de Géodynamique et de Séismologie* 17, 169-175.
- IV. Virtanen H., 2001. Hydrological studies at the gravity Station Metsähovi in Finland. *Journal of the Geodetic Society of Japan* 47 (1), 328 - 333.
- V. Virtanen, H., Mäkinen, J., 2003. The effect of the Baltic Sea level on gravity at the Metsähovi station, *Journal of Geodynamics* 35/4-5, 553-565.
- VI. Virtanen, H., 2004. Loading effects in Metsähovi from the atmosphere and the Baltic Sea, *Journal of Geodynamics* 38/3-5, 407-422.

Paper [I] investigates free oscillations of the Earth, observed after the major earthquake (Mw 8.2) in Kuril Islands on October 4th, 1994. Paper [II] studies the characteristics of microseismic and seismic background noise in Metsähovi. Papers [III] and [IV] analyse the gravity effects of hydrological phenomena, such as variation in groundwater level, precipitation, soil moisture and snow cover. Papers [V] and [VI] examine the gravity effect of the variation in atmospheric mass, and of the loading by the Baltic Sea. They utilize both regression methods based on a single tide gauge/barometer, and calculations with detailed models for the surface loads. Paper [VI] also associates the loading effects with temporal height variations using the GPS data of Metsähovi permanent station.

Papers [III, IV, V and VI] have been peer reviewed. Papers [I, II, III, IV and VI] were written by me alone. Paper [V] was written together with J. Mäkinen. I took the initiative, processed the gravity data, and made the loading calculations and the graphics. J. Mäkinen contributed statistical and oceanographic knowledge. The final version was then produced together.

To provide the necessary background, this review first gives the description of the SG installation, data acquisition and processing. Then the investigations in the papers [I-VI] are summarized, updated and complemented where needed. Some relevant new results, e.g. tidal analyses are given.

1. Introduction

1.1. Superconducting gravimeter as a research tool

The superconducting (or cryogenic) gravimeter is based on the levitation of a superconducting sphere in a stable magnetic field created by current in superconducting coils (Prothero and Goodkind, 1968; Warburton and Brinton 1995; Goodkind, 1999). Depending on frequency, it is capable of detecting gravity¹ variations as small as 10^{-11}ms^{-2} . For a single event, the detection threshold is higher, conservatively about 10^{-9}ms^{-2} . An SG can also be used as a long-periodic seismometer (Widmer-Schmidrig, 2003).

Due to its high sensitivity and low drift rate, the SG is eminently suitable for the study of geodynamical phenomena through their gravity signatures (Hinderer and Crossley, 2000; Jentzsch, et al. 2004). The process is recursive: the gravity record is corrected for known effects, in order to reduce noise and detect smaller and smaller phenomena.

The superconducting gravimeter GWR T020 (Fig. 1.1) has worked continuously in Metsähovi, Finland since August 1994 (Virtanen and Kääriäinen 1995; 1997). Metsähovi is a multi-technique geodetic laboratory including absolute gravity, permanent GPS, GLONASS, satellite laser ranging, DORIS beacon and geodetic VLBI. They are influenced by the same environmental effects as the SG. With its high sensitivity, the SG is an excellent tool for testing and validating the pertinent correction models.

The T020 is a part of the GGP network (Crossley et al., 1999). The GGP worldwide network (Fig. 1.2) consists of 20 working stations (status June 2005). Station are concentrated in Europe and Japan. The first phase of the project was 1997-2003, continuing as phase 2 (2003-2007). The achievements of phase 1 were published in a special issue of Journal of Geodynamics (Jentzsch et al., 2004). The data of the T020 and of other participating SGs are available to the scientific community through the GGP-ISDC (Global Geodynamics Project Information System and Data Center) at GFZ.

One of the original goals of the GGP is the detection of the translational motion of the solid inner core, or the Slichter triplet, in the sub-seismic band. Its periods due to rotational splitting constrain the density contrast at the inner core boundary, and even its viscosity (Smylie et al., 2001). Despite low noise levels in the band from 3 to 6 hours and advanced methods (e.g. stacking), the detection is still an open challenge to GGP community (Hinderer and Crossley, 2004)

Although the SGs only provide point measurements, comparisons with the regional gravity variations observed with the satellites CHAMP and GRACE have proved fruitful (Crossley and Hinderer, 2002; Crossley et al., 2004; 2005; Neumeier et al. 2004; 2006). This will be discussed in Section 6.3.

1.2. Temporal variation in gravity

SG observes the vertical component of gravity, and the vertical acceleration of Earth surface. The temporal variation in gravity consists of numerous phenomena with different periods and amplitudes. Earth tides have the strongest effect, in ME about $2250 \times 10^{-9}\text{ms}^{-2}$ peak to peak (p-p). The next largest is the variable gravity effect of the atmosphere. The range of atmospheric pressure at ME is about 100 hPa, corresponding $300 \times 10^{-9}\text{ms}^{-2}$ in gravity. The pole tide in ME is $80 \times 10^{-9}\text{ms}^{-2}$ (p-p). Hydrological phenomena such as

¹ In this review SI units are used. However, in some of the Papers occasionally the cgs-unit “gal” was used ($1\text{gal}=10^{-2}\text{ms}^{-2}$, $1\mu\text{gal}=10^{-8}\text{ms}^{-2}$, $1\text{ngal}=10^{-11}\text{ms}^{-2}$)

variation in soil moisture content, groundwater level and snow cover have an influence up to $80 \times 10^{-9} \text{ms}^{-2}$. The loading effect of the Baltic Sea varies about $40 \times 10^{-9} \text{ms}^{-2}$ (p-p). An extensive review of environmental effects of gravity is given by Van Dam and Wahr (1998).

The ground acceleration due to strong earthquakes exceeds all magnitudes above. The effect of a strong microseism (MS) can be about $1000 \times 10^{-9} \text{ms}^{-2}$. Weakest observable periodical phenomena, such as free oscillations of the Earth are $0.01 \times 10^{-9} \text{ms}^{-2}$ in amplitude (Chapter 3).



Fig. 1.1. Superconducting gravimeter T020 in gravity laboratory at Metsähovi.

2. Installation and data processing

2.1. Site description

The SG T020 was installed in a specially designed gravity laboratory at Metsähovi in August 1994. The building and the gravimeter pier stand on a knoll of Precambrian granite. The T020 is equipped with a 200 litre Dewar for liquid helium. Technical details are given by Warburton and Brinton (1995) and in the GWR operating manual (GWR, 1989). A general description of the T020 system, gravity laboratory and DAS (until July 2003) is given by Virtanen and Kääriäinen (1995;1997).

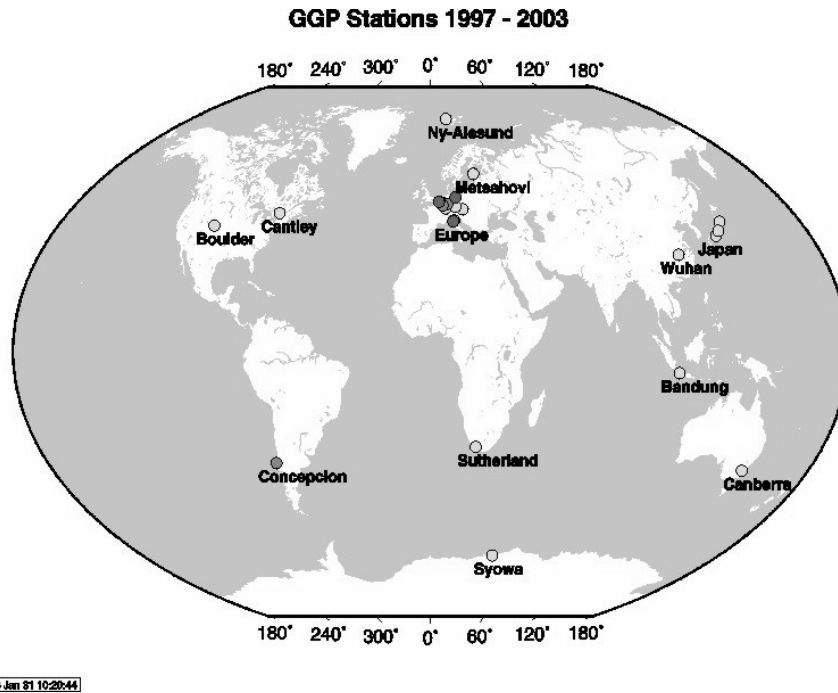


Fig 1.2. GGP network of SG stations on June 2005. New stations in Taiwan and South Korea are not shown.

The coordinates of the site are $\varphi = 60.2172$ N, $\lambda = 24.3958$ E and the height of sensor is 55.6 m above the sea level in the Finnish N60 height system. The station is located in a rural area. There are no industrial plants or transport arteries that could cause ground vibrations. Among the GGP stations ME belongs to the group with low seismic background noise (Chapter 3). The surroundings are relatively flat: the range of heights is 46 – 56 m within 100 m of the station and 35-73 m within 1000 m. The building is on exposed bedrock. The overburden is thin: the average within 100 m of station is 0.8 m and the maximum about 3 m. The building was surrounded by forest until two storms in 2001 and 2002 felled the trees and now it is in an open area.

The T020 is not equipped with automatic tilt control. Abrupt temperature changes in the laboratory can tilt the gravimeter. We have kept the temperature nearly constant at 23°C using a thermostat and an electric heater. However, during summer the temperature in the room can exceed this limit. Interruptions in the cooling system change the temperature of the gravimeter neck, causing it to tilt. Short terms disturbances in the gravity record can in these cases reach 20 nms^{-2} . The desensitization (checking the tilt minimum) of the T020 has been performed regularly. On the basis of test computations it was decided not to correct gravity data using the tiltmeter records (Virtanen and Kääriäinen, 1997).

2.2. Operating history

The gravimeter itself has been working continuously since installation in August 1994, but malfunctions of the DAS have caused about ten interruptions in the registration. Typically gaps were a day or two. The second longest gap was two weeks. The longest gap was caused by a thunderbolt, which destroyed the GPS receiver of the installation on July 5, 2003. It was necessary to develop a new DAS (Section 2.5) before the registration could be restarted in November 2003. This data gap lasted 4 months (Fig. 2.1). Disturbances in the cooling system have caused some rejection of data in analysing stage (Section 2.4).

In September 1997 the original gravity card was replaced by a new one called GGP1, following the recommendation of the GGP project (GGP 2006). The main difference between the cards is the corner frequency in low pass filtering, which is 40 s for the original card and 16.3 s for the GGP1, which make better possibility to study microseism [II]. During repair of the GGP1, the old card was again used from March 16, 1999 to January 3, 2001.

2.3. Calibration

The T020 was calibrated using simultaneous observations with the absolute gravimeter JILAg-5 in 1995 (Mäkinen et al., 1995; Hinderer et al., 1998). We have adopted the value $1107 \pm 3 \text{ nms}^{-2}\text{V}^{-1}$ (one sigma) Thereafter calibration has been checked occasionally. To obtain a large tidal amplitude, the calibrations were carried out near new or full moon. Typically, 2400 drops in the absolute gravimeter per day were carried out, the whole calibration lasting 3-5 days. The latest calibration was made with the absolute gravimeter FG5-221 in June 2005. The later results were compatible with the original value within the error limits.

Some comparisons with ocean loading models seem to indicate that the value above is too high by 0.3 % (i.e. by its standard error). This will be discussed in Section 4.1. A unified recomputation of all calibration observations accumulated over the years is in progress. The results presented in papers [I-VI] do not in practice depend on the calibration factor.

Transfer functions were measured and calculated for the original and for the GGP1 gravity card in September 1997 using the method described by Van Camp et al. (2000). In the tidal band the lag was 16.6 s and 9.5 s for the original and for the GGP1 card, respectively (0.0690 and 0.0395 deg/cpd).

In addition to gravity, special attention has been paid to the accuracy of the barometers (Virtanen, 2003).

2.4. Data processing

For uniformity, all gravity data, originally processed in shorter batches were reprocessed several times from 1996 to 2005. The current data processing methods are described in detail in papers [V and VI] and by Virtanen and Mäkinen (2003). The description will be not repeated here. The data set of paper [VI] ends August 31, 2002. The same set is used in Chapters 4 and 5. For the paper by Neumayer et al. (2006) and for Chapter 6 the data set was extended to July 4, 2003. Some stages of data processing are presented in Figures 2.1, 2.2 and 2.3. Fig 2.1 shows the raw T020 record without any corrections, only the calibration factor has been applied. In Fig. 2.2 tides, pole tide and air pressure corrections have been subtracted. Steps and spikes are well visible and the figure demonstrates the importance of and the difficulties in eliminating drift and offsets, especially for long-term studies. Fig. 2.3 shows the final gravity residual after spikes, offsets, traces of big earthquakes etc. were removed, the groundwater effect corrected for,

and drift eliminated in three separated blocks (Section 4.3). The pole tide has been restored to the graph to demonstrate the successful preparation of data. The TSOFT 2.0.15 program package (Van Camp and Vauterin, 2005) was used in the correction processing and analyses.

The apparent drift rate for the last block of data starting September 1, 2000 was $+31 \text{ nms}^{-2}(\text{yr})^{-1}$. The secular gravity change at the site is about $-10 \text{ nms}^{-2}(\text{yr})^{-1}$ according to the co-located absolute gravimeter record (JILAg-5) and is thought to be due to postglacial rebound. The net drift of the T020 is thus about $40 \text{ nms}^{-2}(\text{yr})^{-1}$.

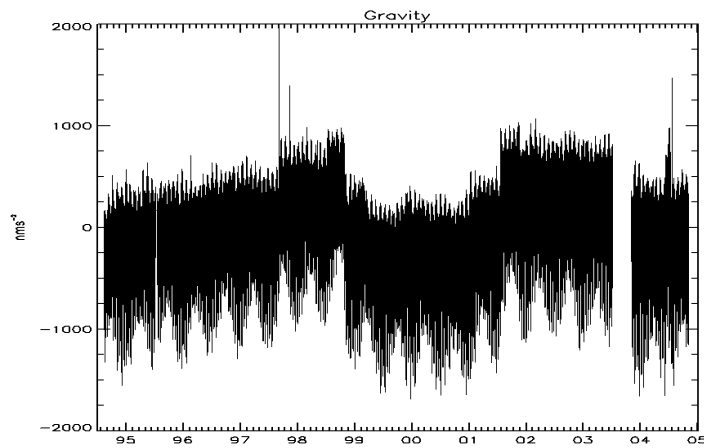


Fig. 2.1. Gravity data by obtained with T020 at Metsähovi from 12th August 1994 to 1st November 2004.

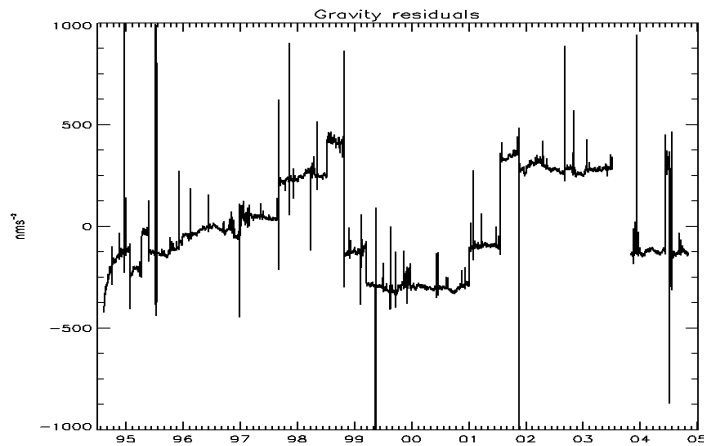


Fig. 2.2. Gravity residuals by T020 shown at Metsähovi 12th August 1994 – 1st November 2004. Tide, pole tide was subtracted and air pressure correction was made by coefficient of $3.10 \text{ nms}^{-2}\text{hPa}^{-1}$.

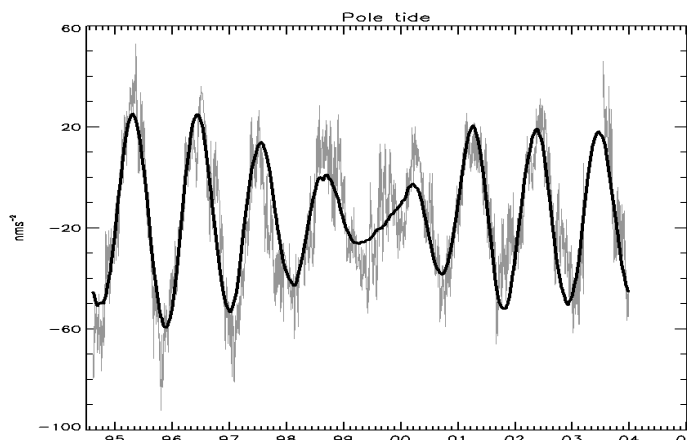


Fig.2.3. Gravity residuals at Metsähovi from 1st December 1994 to 17th April 2004 (thin grey line) and pole tide with amplitude factor 1.16 (thick black line). Tide and groundwater effect was subtracted and air pressure correction was made by coefficient of $3.10 \text{ nms}^{-2} \text{ nms}^{-2} \text{ hPa}^{-1}$.

2.5. The new data acquisition system

The original data acquisition system (DAS) was based on the CSGI software (Dunn, 1994) running since 1994 on a PC with the QNX® operating system. The system was damaged during a thunderstorm in July 2003. The GPS receiver was destroyed and it was not possible to find a replacement that could be operated using the protocol (“silent TSIP”) required by the CSGI. Hence, it was necessary to develop quickly an adequate DAS.

The recording was restarted in November 2003 using a temporary version of the new system. It used a single PC (PC1) with the Windows 2000® operating system. The HP3457A digital voltmeter from the original system is still used to record gravity. It has precision of 7.5 digits (24 bits) and good long-term stability. It is hardware triggered every second (pps) by GPS (Trimble). In this first version commercial PDAQ55 (USB data acquisition module) was used to record the main auxiliaries, such as air pressure, groundwater precipitation and Dewar temperature, which are sampled every second.

The system was completed with second PC2 in the summer of 2004. In this final version the main task of PC1 is gravity recording while PC2 records environmental and instrumental quantities. For this it uses the multiplexing digital multi-meter HP3421A from the original DAS. The HP3421A with 5.5 digits precision includes 18 data channels. Both HP instruments are controlled by the GPIB bus through adapters HP82357A, connected to the USB ports of the computers. Actually the voltmeters reproduce the original DAS with the same connection wiring.

The adapters are equipped with an extensive I/O library and source code for applications “VISA” (Virtual Instrument Software Architecture). The voltmeters are controlled and data acquired with programs “high_res” (HP3457A) and “hp_dacu” (HP3421A). The programs were written by the author around modules of VISA source code using standard (ANSI) C-language and libraries. The PDAQ55 was retained and is now connected to PC2. It provides a flexible method to record additional auxiliaries and to plot them on the screen.

As previous mentioned, gravity measurements on PC1 are hardware triggered by GPS one-second pulse to voltmeter. The sampling rate for auxiliary data on PC2 is 10 seconds

and it is software triggered by PC clock. Both computers keep correct time via an Internet connection to NIST time servers (e.g. time-b.nist.gov) every 10 minutes. In addition, PC1 is equipped with a DCF radio clock which updates the PC clock every minute. The accuracy of the PC's timekeeping is typically 10 ms for PC1 and 20 ms for PC2. All recorded samples include time and date stamps by PC's clock.

The most important files such as gravity and air pressure are stored in ASCII format and the files are identified as "yydoy.xxx" (year and day of year). Both PC1 and PC2 are connected to the Internet and to the intranet of FGI. Gravity and pressure files can be downloaded at any time, even while they are still being written. The hard disk space is sufficient for several years of recording.

The computers are similar standard PC devices. All connections are made using USB and standard serial ports, no special pc-boards are required. All important software are installed in both computers. Thus an adequate DAS can quickly be built on a single computer using only part of the full DAS. This reduces the risk of long data gaps in the case of computer or other device failure.

Another basic principle in the system design is the remote control. Authorized remote computers can control systems via VNC (Virtual Network Computing). The computers are fully remote controlled including boots.

The screens of both computers are shown in Figs. 2.4 and 2.5. The letters in brackets refer to these Figures. Screen dumps of both computers are sent every 5 minutes to the ftp server of the FGI. Screen outlooks are seen everywhere later on. We have included some useful features on the screens. PC1 plot [A] gives the spectrum of 1 second gravity data from 10 mHz to 500 mHz, updated every ten second. This window gives at a glance information for MS, surface waves after earthquakes and the general quality of data.

The screen of PC2 [B] shows the gravity output after MODE and TIDE filters and is updated every minute. The MODE filter is a bandpass filter, periods about 1 min-60 min (GWR, 1989). This signal is amplified by 20. The TIDE filter is a lowpass filter with cut-off at 50 seconds. Both outputs are visible in the window, which show the last 48 hours. The TIDE curve shows output of gravimeter in tidal band and the MODE curve reveals disturbances, e.g. earthquakes. The plotter programs use the IDL Virtual Machine™ utility. Other windows show selectable outputs of the PDAQ55 data acquisition unit [A], E] and [F]. This device includes a pulse counter, which is connected to the rain gauge [E]. The device has free channels and if necessary, further expandability. PC2 reads altogether 18 channels [B] including environmental and instrumental temperatures, air pressure and groundwater, TIDE and MODE signals.

The PC1 has a ftp server and PC2 has the controlling programs for the UPS. The full DAS consists of many independent pieces, and restarting the entire system is a somewhat laborious task. On the other hand updating and modification of system parts is more simpler and an interruption of the whole system is not necessary. The DAS as a whole has proved to be reliable and flexible. Most importantly, the accuracy of the data and of the timing are good enough for SG.

Due to the importance of air pressure registration, we aim to record more than one barometer at all time. The sensors outside the laboratory are typically related to environmental phenomena, such as groundwater level and precipitation (Chapter 6).

On the screen of PC2 one can see the effects of the great earthquake in Sumatra 26.12.2004 UT 00:58 (M9.0). The window [A] shows an exceptionally strong horizontal acceleration due to the surface waves recorded with the tiltmeters of the SG.

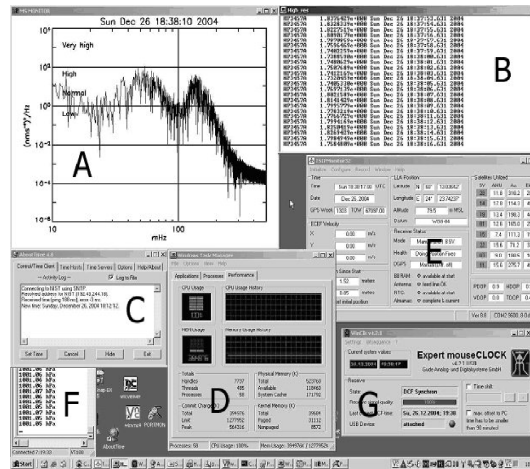


Fig 2.4. The screen of the computer PC1. [A] MS MONITOR, (IDL VM™), 10s updating, One hour spectrum for one second data of window [B]. [B] Output of "High_res" (C-language) program, 1-second, 7.5 digits high-res resolution gravity data taken with HP3457A voltmeter triggered by GPS (pps). [C] Output window internet timing, automatically updated every 10 minutes. [D] Control window for computer system. [E] The program "TSIPMON32" is needed to start the GPS pps operation. [F] Output of the digital barometer (Vaisala) PTB220, one second samples. [G] DFC radio clock, PC-time to atomic time every minute.

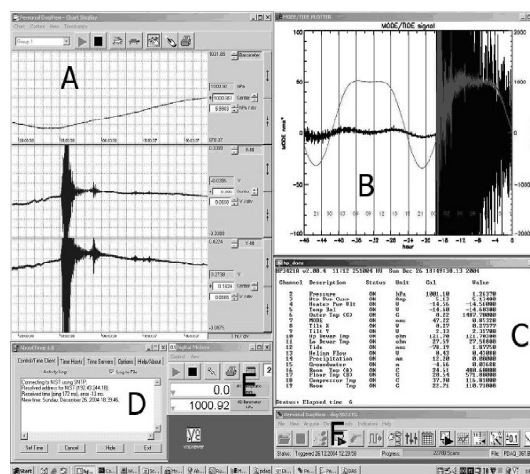


Fig 2.5. The screen of the computer PC2. [A] Chart display of PDAQ55 (one second samples). Speed and channels are selectable. In this case air pressure, tilts of SG (x and y) are shown, 24 hours are visible. [B] MODE/TIDE PLOTTER (IDL VM™), 1-min updating, data sampled every 10 seconds, last 48-hours are visible with fixed and running time axes. [C] Output of "Hp_dacu" (C-language) program, 18 channels are sampled every 10 seconds, accuracy is 5.5 digits. [D] Internet timing output window, automatically updated every 10 minutes. [E] Main control window of the PDAQ55 data acquisition module. [F] Digital output of PDAQ55, in this case air pressure and precipitation are shown. Air pressure is the analog output of the digital barometer PTB220.

3. The seismic frequency band

3.1. Seismic background noise

A special concept “Seismic Noise Magnitude” (SNM) has been developed to give an unambiguous measure of background noise level at any gravity stations (Banka and Crossley, 1999). It is based on the Power Spectral Density (PSD) calculated from the mean FFT in the period range 200-600 s. The 5 quiet days of gravity data has been used for SNM (GGP, 2006). It is defined as:

$$SNM = {}^{10}\log(\text{mean PSD}) + 2.5$$

For ME the SNM factor is 0.88. It varies from 0.20 (Moxa in Germany, SG CD034) to 2.20 (Brasimore in Italy, SG T015). Later comparisons of the seismic noise levels at various GGP stations were made by Rosat et al., (2002) and Rosat et al., (2004). The investigations covered the spectrum between 200 s and 24 h (Rosat et al. 2004). Among 20 SG stations, ME has the 8th lowest noise magnitude and it belongs to group of low noise stations. Thus, ME is a very suitable station for studies in the seismic frequency band. Fig 3.1 presents the PSD of the spectrum from 0.01 mHz to 1000 mHz for three days. The densities are determined in a similar way as in Banka (1997). This figure updates older background noise presentations (Fig 14 in [II]). The upper graph shows the spectrum during quiet days and using the original gravity card (Section 2.2). The MS-band (from 66 mHz to 500 mHz) is strongly attenuated by the low pass filter. The data for next two spectra were taken with the GGP1 gravity card. The middle graph gives the spectrum during strong MS, periods for peaks are about 12 seconds and 6 seconds. The bottom graph represents the spectrum on a quiet day. The thick line indicates the level of New Low Noise Model, often referred as NLMN (Peterson, 1993).

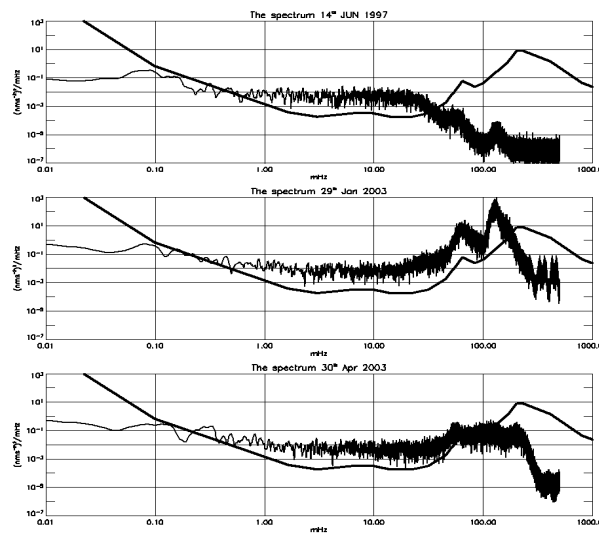


Fig. 3.1. The Power Spectral Densities from 0.01 mHz to 1000 mHz for one day. Top: Old gravity card and low MS level (June 14, 1997), Middle: New gravity card and high MS (January 29, 2003), Bottom: New gravity card (GGP1) and low MS level (30 April 2003).

3.2. *Microseism*

The paper [II] analyses of ME data at periods shorter than 2 minutes (over 8 mHz). This limit was chosen, because for most applications we use the data filtered to 1 minute. The paper presents information on the nature of microseism (MS) at Metsähovi. Annual variations, spectral distributions, amplitudes and sources are given.

There is a clear correlation between the occurrence of low atmospheric pressure (storm) in the Northern Atlantic Ocean and MS. The usual shape of the spectrum shows two peaks near 12 and 6 second periods. However, the location of the peaks varies with the source. Typical examples are the Norwegian coast and the middle Atlantic Ocean. In addition, distant medium size earthquakes are treated as seismic noise. The amplitude of ground motion can exceed 0.003 mm during a strong MS. In paper [II] moving window spectrum for frequencies up to 300 mHz was presented from 10 August 1994 to 28 October 1998. The effect of changed gravity card (filter cut-off changed) is clearly seen from 5 September 1997. As to the seasonal variation, the period from April to September has rather low MS and the strongest MS storm occurred often between January and March.

In SG studies outside the seismic band, the MS is generally not a source of uncertainty, due to the filtering. However other gravity observations (absolute and relative) suffer from MS and may benefit from insights gained with the SG.

3.3. *Free oscillation of the Earth*

The paper [I] presents observations of the free oscillation of the Earth after the great earthquake in Kuril Islands on 4th October 1994. The spectra were calculated using two methods: Lomb-Scargle periodogram and FFT. We had 1-minute gravity data, corrected for air pressure and then used a high pass filter (one hour cutoff). We were able to extract clearly the lowest spheroidal mode ${}_0S_2$ (0.30945 mHz, or 54 minutes). Zürn et al. (2000) noticed this rare observation and the success of air pressure correction in seismic band. In addition, I presented the attenuation and duration of other spheroidal modes. We were able to detect radial mode ${}_0S_0$ (0.81439 mHz or 20 minutes) above level of one nanogal (10^{-11}ms^{-2}) over six weeks. Others modes disappeared during two days. In addition, graphics of the two dimensional summary was presented from August 1994 to August 1996. [I, p. 430]. We can say that the excitation ${}_0S_0$ mode has been observed at the one ngal level at least 25% of total recording time.

Another significant great earthquake (magnitude 8.4) occurred in Peru on June 23, 2001. This quake excited the “football mode” ${}_0S_2$ with quite high SNR (Widmer-Schmidrig, 2003). The lowest modes of this quake with T020 are shown in the spectrum of 72-hours in Fig. 3.2. The gravest toroidal mode ${}_0T_2$ (0.37730 mHz, or 44 minutes) is clearly discernible. This mode is very seldom detected with vertical instruments as it influences then through Coriolis coupling only. Individual singlets of the ${}_0S_2$ mode are presented in Fig. 3.3 (0.30480, 0.30949 and 0.31400 mHz). In the spectrum of shorter time series this rotational splitting complicates observing this mode. The longer time series reveals individual singlets of ${}_0S_2$. On the other hand the mode ${}_0T_2$ disappears. In addition, the splitting of the mode ${}_0S_3$ (0.46855 mHz) is visible.

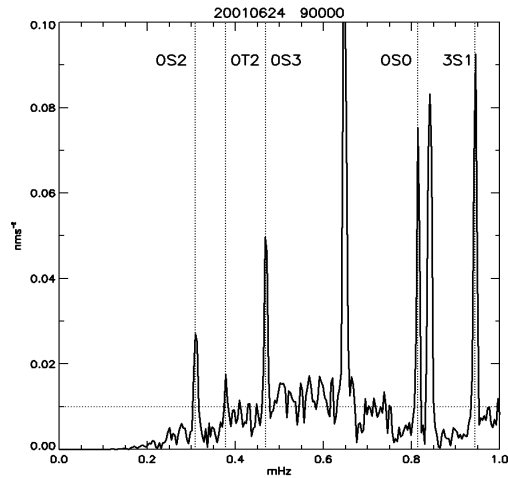


Fig. 3.2. Free oscillation of the Earth. Peru earthquake 23.06.2001 UT 20:45 (Mw 8.4). The length of spectrum is 72 hours, since 24.6.2001 UT 9:00. The gravity 1-min data is hanning windowed, air pressure corrected ($-3.10 \text{ nms}^{-2}\text{hpa}^{-1}$) and high pass filtered (1 hour). The 1 ngal (10^{-11}ms^{-2}) level is shown as dotted line.

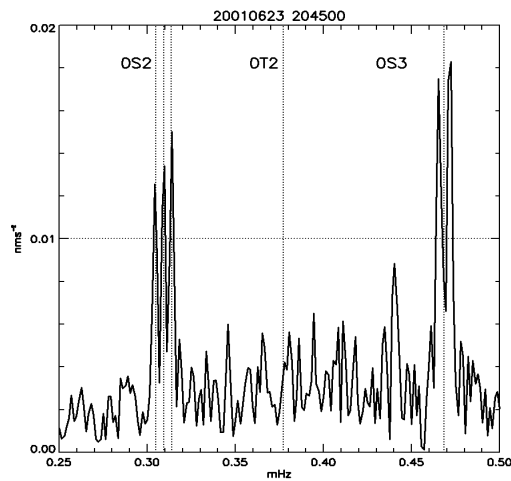


Fig. 3.3. Free oscillation of the Earth. Peru earthquake 23.06.2001 UT 20:45 (Mw 8.4). Splittings of the lowest spheroidal mode ${}_0S_2$ and the mode ${}_0S_3$ are visible. The length of the spectrum is 200 hours, since 23.06.2001 UT 20:45. The gravity 1-min data is hanning windowed, air pressure corrected ($-3.10 \text{ nms}^{-2}\text{hpa}^{-1}$) and high pass filtered (1 hour). The 1 ngal (10^{-11}ms^{-2}) level is shown as dotted line.

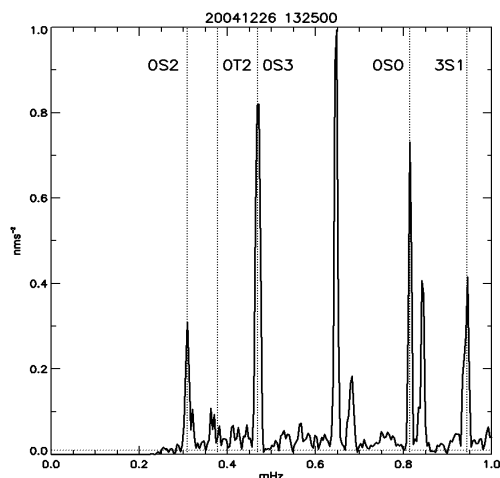


Fig. 3.4. Free oscillation of the Earth. Sumatra earthquake 28.12.2004 UT 00:58 (Mw 9.0). The length of spectrum is 72 hours, since 26.12.2004 UT 13:00. The gravity 1-min data is hanning windowed, air pressure corrected ($-3.10 \text{ nms}^{-2}\text{hpa}^{-1}$) and high pass filtered (1 hour). The 1 ngal (10^{-11} ms^{-2}) level is shown as dotted line.

The strongest earthquake since 1964 occurred in Sumatra beneath the sea on December 26, 2004, UTC 0:58 (NEIC, 2005). Its magnitude was 9.0 and it caused a destructive tsunami. Fig. 3.4 represents the same time span after the quake as to Fig. 3.2. The amplitude of ${}_0S_2$ (30 ngal) seems to be 12 times greater as in Peru earthquake 2001. This quake did not bring forth the toroidal mode ${}_0T_2$, due to differences in fault mechanism. The amplitude of ground motion due to the mode ${}_0S_0$ was a few days after the quake about 0.05 mm, exceeding 10 times the amplitude of strong MS. In the beginning of February 2005 the amplitude was still 0.02 mm. This mode was clearly detectable above the noise as long as three months after the quake (Fig. 3.5). The amplitude was at the end of March about 2 ngals. Unfortunately the noise level in this data was high due to disturbances in the cooling system. It was not possible to analyse the splitting of modes.

3.4. Incessant excitation of the Earth's free oscillation

A special phenomenon that has been discovered with superconducting gravimeter is the incessant excitation of the Earth's free oscillation, now colloquially called the 'hum'. This phenomenon was first found at Syowa station in Antarctica (Nawa et al., 1998) and is also observed from data of T020 among other SG records (Nawa et al., 2000). Fig. 3.6 shows this continuous excitation of free oscillation modes with T020 from August 1994 to August 1998. The amplitude is on the order of 1 ngal. The normal modes are seen as fuzzy dark horizontal lines, and strong quakes as clear vertical lines. Normally after a strong quake the modes are excited clearly and then they disappear in two days. The origin for this low level excitation is still not clear but the best candidates appear to be the atmosphere or ocean (Hinderer and Crossley, 2004).

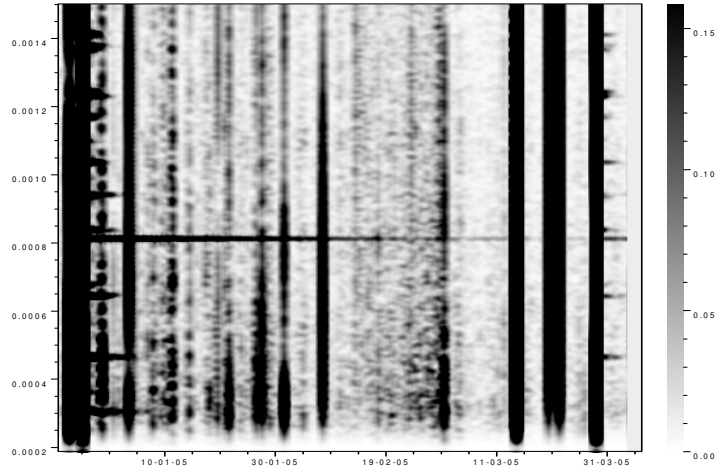


Fig. 3.5. Moving window spectrum from 22 December 2004 to 5 April 2005. 1-min data, hanning windowing, air pressure corrected and high pass filtered. The length of window is 4096 minutes and shift 128 minutes. Horizontal axis gives time and vertical axis show frequencies in mHz. Vertical dark lines are strong earthquakes. Radial mode ${}_0S_0$ is seen in the middle. The mode was excited again 28 March 2005 by the earthquake in northern Sumatra (Mw 8.7).

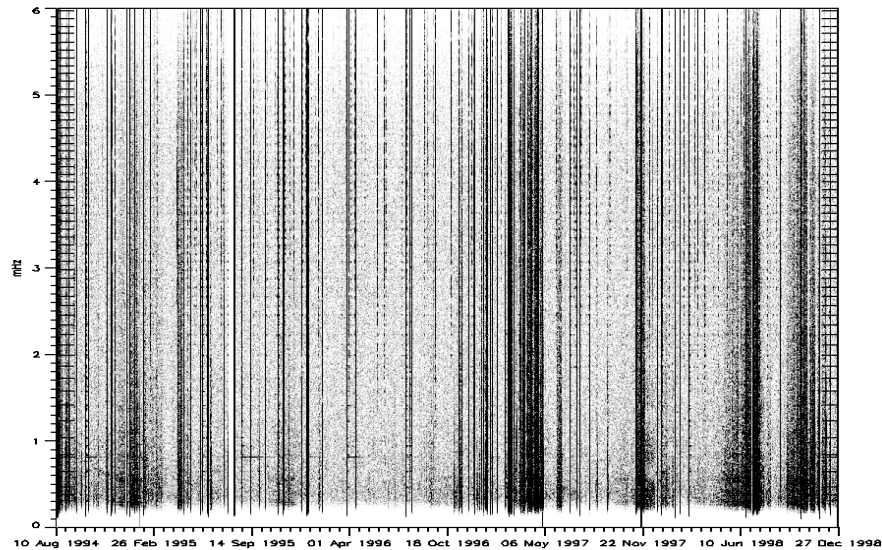


Fig. 3.6. Incassant free oscillation of the Earth recorded with the T020. The horizontal axis gives time from August 1994 to December 1998. The vertical axis shows a frequency in mHz. The frequencies of normal modes are marked inside of y-axis. The scale is linear and the excitation is seen as fuzzy horizontal lines. Sharp dark vertical lines due to strong earthquakes and other disturbances are seen as darker background.

4. The tidal frequency band

4.1. Tidal models at Metsähovi

One of the most important tasks in SG data processing is to remove the tidal effect from gravity to study other weaker phenomena. Results of tidal analyses are applied for this purpose. An accurate local model is needed instead of some general model. The difference between gravity residuals from local and Wahr-Dehant models (Wenzel, 1996, Dehant et al., 1999) can in longer time series be up to 10 nms^{-2} . An example of the effect different tidal models on the standard deviation of gravity residuals is given in chapter 5. On the other hand, tidal analyses are used to obtain information about elastic properties of the Earth and to study and validate ocean tide models. In the framework of the GGP several authors have used the data of ME in their studies. In addition, the ICET regularly publishes tidal analyses for different stations using the GGP databank. Baker and Bos (2001;2003) corrected observed amplitudes of O1 and M2 for different ocean loading models. They found that observed amplitudes were too high by 0.3 % compared to the Wahr-Dehant model and concluded that this could be due to the error in the calibration. Note for uncertainty of calibration was quoted in Section 2.3. Similar conclusions were presented by Ducarme et al., 2001;2002, Xu et al., 2004). However Boy et al. (2003) found that discrepancy could also be explained by inaccuracies in ocean tidal models (e.g. the Baltic Sea and the Arctic ocean). Large calibration errors were concluded by Arabelos (2002). However, this work is based on the very first tidal analysis by Virtanen and Kääriäinen (1995). It uses only 113 days of data and no conclusion can be drawn from it.

In Table 1 we present results for waves O1 and M2 from ICET and by the author. In the Table 2 we give results of two analyses for K1 and PS1 waves, which are strongly affected by Near Diurnal Resonance. In the Tables 3 and 4 we give results with long periodic tides. In these analyses results are greatly depending on drift modeling and using local groundwater and Baltic Sea level as regression parameters.

In the Appendix 1 we give tidal parameters for the local tidal model used in works presented in papers [III-VI]. In Appendices 2 and 3 we show newer results of tidal analyses for ME data. All analyses were carried out with the ETERNA program package (Wenzel, 1996).

Table 1

Standard deviation and tidal factors for O1 and M2 for different data sets of T020 at Metsähovi.

No	Source	Length	STD	AP	Error	O1(δ)	Error	O1(α)	Error	M2(δ)	Error	M2(α)	Error
1	ICET	538	0.759	-3.690	0.007	1.1532		0.25		1.1818		0.73	
2	ICET	2333	1.225	-3.653	0.006	1.15294	0.00013	0.2533	0.0067	1.18093	0.00008	0.7071	0.0039
3	Author	2620	0.971	-3.647	0.004	1.15321	0.00011	0.2618	0.0053	1.18133	0.00006	0.7079	0.0028
4	Author	690	0.866	-3.811	0.008	1.15364	0.00004	0.2635	0.0022	1.18219	0.00005	0.7123	0.0025
5	Author	690	8.487	-3.031	0.006	1.15347	0.00035	0.2585	0.0173	1.18218	0.00011	0.7115	0.0051
6	Author	2620	8.542	HIRLAM		1.15488	0.00012	0.2400	0.0061	1.18086	0.00006	0.7016	0.0031

Lengths are given in days. STD is “standard deviation of gravity residuals” as nms^{-2} . AP is obtained air pressure admittance ($\text{nms}^{-2}\text{hPa}^{-1}$). Rows 1-4 are based on high-pass filtered data and only periods up to diurnal are determined. Longer than diurnal tides are included in analyses shown in Rows 5 and 6. Row 1 (August 1994 – January 1996) was calculated at ICET (Ducarme and Vandercoilden, 2000) and results (δ) was used by Baker and Bos (2001; 2003). Row 2 gives results of model “00200892.we3” on the ETGGP #5a distribution disk (GGP, 2003) including August 1994 – June 2002. Row 3 gives (ME03) results December 1994 – August 2002. The data are the same as in Paper [VI]. The data

processing and analyses were made by the author. Fig. 4.1 shows the spectrum of gravity residuals after this analysis. All tidal parameters are shown in Appendix 3.

Results in Row 4 are based on the same data as Row 5 (November 1994 – October 1996) and gave the LTM used in Papers [III-VI]. The analysis in Row 5 includes long periodic tides. However, in the actually used LTM (ME01, Appendix 1) we have used a priori values ($\delta=1.16$ and $\alpha=0.00$) for SA and SSA waves.

Row 6 gives results for the same data as used in Row 3, however, including long periodic tides too. This model is referred as ME02. Air pressure effect was corrected with HIRLAM, and HSL (Helsinki Sea Level) was used as a meteorological or a hydrological parameter. The procedure of air pressure corrections is explained in detail in Paper [VI]. Complete results are given in Appendix 2.

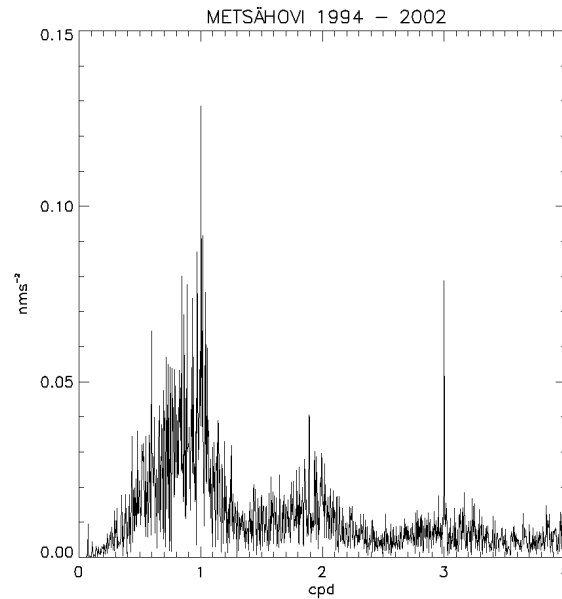


Fig 4.1. Amplitude spectrum of gravity residuals for ME03.

Temporal stability of different data sets for tidal factor (δ) are calculated to be $< 0.1\%$, when comparing two data sets (1994-1996 and 1997-2000) and waves O1, K1, M2 and S2 at ICET (Ducarme et al., 2002)

GGP data has been used for determinations of FCN parameters (Free core nutation). The obtained eigen periods comprised between 429.1 and 429.9 days, converging towards value 429.5 days reduced from VLBI observations (Ducarme et al., 2002, Sun, et al. 2002a, Sun, et al. 2002b). For ME the value of 430.6 has been obtained (Sun et al. 2002a). As an example the Table 2 shows results of two analyses for waves K1 and PSIII. These waves are strongly affected by the near diurnal resonance.

Table 2
Results (T020) for waves K1 and PSII, which were analysed at ICET and by author.

No	Source	K1(δ)	Error	K1(α)	Error	PSI1(δ)	Error	PSI1(α)	Error
2	ICET	1.14051	0.00009	0.0695	0.0046	1.25887	0.01096	0.5158	0.4990
3	Author	1.14055	0.00007	0.0793	0.0036	1.25783	0.00868	0.4927	0.3954

4.2. Long period tides

For the time series (December 1994 – August 2002) presented in Row 6 of Table 1, we have analysed long period tides (SA, SSA and STA). This is the same data set as in Paper [VI]. Various treatments were carried out with auxiliaries, such as local air pressure, HIRLAM grid, groundwater level and Baltic Sea level. The drift correction models are closely related to these analyses.

Table 3

Result of long periodic tides (waves separated). In these analyses we have included determinations of groundwater and sea level. Explanations for different treatments are given in text. AP means air pressure coefficient $\text{nms}^{-2}\text{hPa}^{-1}$, next columns are δ -factors for SA, SSA and STA waves. GW means groundwater admittance $\text{nms}^{-2}\text{m}^{-1}$. HSL is Baltic Sea level at Helsinki. Errors in AP are less than last unit.

No	Treatment	RMS	AP	SA(δ)	SSA(δ)	STA(δ)	PT(δ)	GW	HSL
1	AP/PT/GW	10.41	-3.11	1.19	1.24	2.36	1.17	32.31	-
2	AP/PT/GW/HSL	9.36	-2.91	0.95	1.23	1.66	1.16	27.82	25.02
3	PT/GW	10.54	HIRLAM	1.27	1.26	2.58	1.17	33.62	-
4	PT/GW/HSL	9.10	HIRLAM	0.96	1.23	1.64	1.17	28.17	26.28
5	PT/AP	10.11	-3.12	1.43	1.22	2.36	1.14	GW/DRIFT	-
6	PT/AP/HSL	8.82	-2.90	1.09	1.23	1.70	1.13	GW/DRIFT	25.83
7	PT	10.34	HIRLAM	1.54	1.23	2.58	1.14	GW/DRIFT	-
8	PT/HSL	8.54	HIRLAM	1.11	1.23	1.67	1.14	GW/DRIFT	27.12
9	AP	10.27	-3.13	1.18	1.22	2.36	PTCOR	GW/DRIFT	-
10	AP/HSL	8.95	-2.91	0.90	1.23	1.69	PTCOR	GW/DRIFT	26.22
11	NONE	10.53	HIRLAM	1.24	1.23	2.60	PTCOR	GW/DRIFT	-
12	HSL	8.67	HIRLAM	0.91	1.23	1.67	PTCOR	GW/DRIFT	27.67

Explanations for treatments: The letters AP, PT, GW and HSL mean regressions on air pressure, pole tide, groundwater and Baltic Sea level at Helsinki tide gauge respectively. PTCOR means pole tide correction with the fixed factor of 1.16. For treatments 1 - 4 we have used the local groundwater level as a hydrological parameter. The number of blocks for drift in Paper [VI] in this data was 3. However, in these analyses we have used correct phase delays for the whole data, therefore the number of actual blocks is 6. Different phase delays are due to changes of the gravity card. In cases 1-4 we have used polynomials for drift correction as in Paper [VI]. For the first block, degree two was used, for others a linear drift. In other treatments we have corrected both the effect of groundwater and the drift together before analyses. Where air pressure coefficients were given as "HIRLAM", the air pressure correction was made by HIRLAM grid before analyses. Results for treatment 8 are given completely in Appendix 2.

Table 3 shows that the determination of tidal factors for long periodic waves is a very difficult task. There are many environmental phenomena that influence gravity and have an annual and/or semiannual period. Many of them are related to the hydrology.

The Baltic Sea level and air pressure also have an annual behaviour. The results for SA and STA depend completely on the treatment of these phenomena and are in many cases unrealistic. Intriguingly, the results for the semiannual SSA are much more stable.

We have repeated analyses of Table 3 using a single wave group (LPMF) for all periods longer than 4 days (0.00015 cpd – 0.24995 cpd). The results are shown in Table 4.

Table 4
Results for long periodic tide LPMF.

No	Treatment	RMS	AP	LPMF(δ)	Phase(α)	PT	GW	HSL
1	AP/PT/GW	10.88	-3.13	1.16356 \pm 0.00326	0.0178 \pm 0.1613	1.18 \pm 0.34	29.9 \pm 0.1	-
2	AP/PT/GW/HSL	9.80	-2.91	1.16276 \pm 0.00279	-0.3438 \pm 0.1386	1.16 \pm 0.29	28.1 \pm 0.1	23.7 \pm 0.2
3	PT/GW	11.11	HIRLAM	1.16517 \pm 0.00302	0.1889 \pm 0.1487	1.18 \pm 0.32	30.8 \pm 0.1	-
4	PT/GW/HSL	9.53	HIRLAM	1.16351 \pm 0.00252	-0.3259 \pm 0.1254	1.16 \pm 0.27	28.3 \pm 0.1	25.2 \pm 0.2
5	PT/AP	10.58	-3.14	1.16227 \pm 0.00327	0.0319 \pm 0.1616	1.14 \pm 0.31	GW/DRIFT	-
6	PT/AP/HSL	9.21	-2.90	1.16221 \pm 0.00279	-0.2908 \pm 0.1380	1.14 \pm 0.27	GW/DRIFT	25.6 \pm 0.2
7	PT	10.89	HIRLAM	1.16352 \pm 0.00300	0.1778 \pm 0.1477	1.13 \pm 0.29	GW/DRIFT	-
8	PT/HSL	8.94	HIRLAM	1.16285 \pm 0.00252	-0.2810 \pm 0.1248	1.14 \pm 0.24	GW/DRIFT	26.9 \pm 0.2
9	AP	10.66	-3.15	1.16041 \pm 0.00325	0.0210 \pm 0.1607	PTCOR	GW/DRIFT	-
10	AP/HSL	9.38	-2.91	1.15995 \pm 0.00274	-0.2910 \pm 0.1357	PTCOR	GW/DRIFT	24.9 \pm 0.2
11	NONE	10.99	HIRLAM	1.16166 \pm 0.00299	0.1624 \pm 0.1472	PTCOR	GW/DRIFT	-
12	HSL	9.10	HIRLAM	1.16067 \pm 0.00250	-0.2809 \pm 0.1238	PTCOR	GW/DRIFT	26.6 \pm 0.2

Residuals and amplitude factors are smaller using sea level corrections, and the phases change sign. Residuals are generally greater than in Table 3 ($\approx 5\%$). A similar study of long period tides was made by Ducarme et al. (2004). They get for LPMF 1.15246 \pm 0.00317(δ) and 0.302 \pm 0.157(α). After the ocean load correction their results are 1.16945 \pm 0.00317(δ) and -0.427 \pm 0.157(α). Our values (without ocean load correction) are clearly larger. However, Ducarme et al. (2004) do not take into account groundwater or the Baltic Sea. If we do not correct groundwater in treatment no 1 we get $\delta = 1.15268$ (± 0.00378), which is very close to Ducarme et al. (2004). This shows the importance of environmental parameters even in the LPMF approach.

5. Atmospheric effects and the Baltic Sea loading

5.1. Single admittance for air pressure and modeled Baltic Sea

The Paper [V] concerns the effect of the Baltic Sea on gravity at ME. The station is 10 km from the nearest bay of the Baltic Sea and 15 km from the open sea. The tidal variation is of the order of centimeters only, but non-tidal variation of the Baltic is large, up to 2-3 m on the coasts of the Gulf of Bothnia and the Gulf of Finland. Sea level variations in the Baltic are driven at short periods primarily by wind stress, and at longer periods by water exchange through the Danish straits. The loading effect of the Baltic Sea is immediately recognizable in the gravity record of the T020, by simply inspecting residual gravity together with the tide gauge record at Helsinki 30 km away ([V], Fig. 5). Loading calculations show that a uniform layer of water covering the complete Baltic Sea increases the gravity in Metsähovi by 31 nm/s^2 per 1 m of water, and the vertical deformation is -11 mm. We get regression coefficient for short time series (from 6 January to 5 May 2000) 28.8 \pm 0.4 $\text{nms}^{-2}\text{m}^{-1}$, with the correlation coefficient 0.83.

For the whole data (1994-2001) the regression coefficient is 16.6 \pm 0.2 $\text{nms}^{-2}\text{m}^{-1}$, with correlation 0.26. RMS of gravity residuals decreases from 16.6 to 14.0 nms^{-2} . In addition, we calculated the loading effect of the Baltic Sea in ME for 75 models of momentary sea surface (November 15, 2001 – January 27, 2002), using data of 11 tide gauges around the Baltic Sea. For these modelled effects the regression coefficient was 15.7 $\text{nms}^{-2}\text{m}^{-1}$. This study was presented as one of the scientific achievements of the first phase of the GGP (Hinderer and Crossley, 2004).

5.2. Air pressure grid and single tide gauge

In the Paper [VI] we used a longer time series for gravity (1994-2002). This data was completely reprocessed. In the calculation of the air pressure effect, beside local barometer, we have used a grid model (HIRLAM) for air pressure. Regression of gravity residuals on the tide gauge record at Helsinki (at 30 km distance) gives a gravity effect of $26 \text{ nms}^{-2}\text{m}^{-1}$ for the Baltic loading. The correlation coefficient was 0.56. The Paper [VI] demonstrates usefulness of using a grid for a larger area in addition to the local barometer.

5.3. Vertical motion due to loading and GPS

The gravity station is co-located with a permanent GPS station. We have also associated the loading effects of the atmosphere and of the Baltic Sea with temporal height variations. The range of air pressure variations is 100 hPa (940 – 1040 hPa) and the mean is 1004 hPa. The range of modelled vertical motion due to air pressure was 46 mm and that due to sea level 18 mm. The total range was 38 mm. The effects of the Baltic Sea and of the atmosphere partly cancel each other, since at longer periods the inverse barometer assumption is valid. Regression of the modelled height on local air pressure gives $-0.37 \text{ mm hPa}^{-1}$, corresponding approximately to width 6° for pressure system, which is imposed on the actual land-sea geometry of Scandinavia (Scherneck, 1994).

We have tested the models using one year of daily GPS data. Multilinear regression on local air pressure and sea level in Helsinki gives the coefficient $-0.34 \text{ mm hPa}^{-1}$ for pressure, and -11 mm m^{-1} for sea level. These match model values. Loading by air pressure and Baltic Sea explains nearly 40 % of the variance of daily GPS height solutions.

5.4. The effects of different tidal models

Table 5 gives results of new studies correcting gravity for atmospheric and Baltic loading. The table is the similar to Table 2 [VI], but we demonstrate the effect of a different tidal model used in the pre-processing. We have replaced the tidal model ME01 (Appendix 1) originally used with the new model ME02 (Appendix 2). See Section 4.1.

Comparing to the reference GR310, we have reduced residuals (GR HRL /HSL) 16%. Using the original tidal model (ME01), the reference RMS was 10.91 nms^{-2} . Using this reference, the reduction is 18%. For model ME02 we have corrected air pressure effect by HIRLAM grid and used Helsinki tide gauge as a hydrological regression parameter. Drift correction was made before analysis using polynomial fit together with groundwater [VI]. For comparison, using Wahr-Dehant models (Wenzel, 1996, Dehant et al., 1999), the RMS of gravity (GR310) is 12.94 nms^{-2} . Examples demonstrate the importance of accuracy of the local tidal model used.

Table 5

Recalculated Table 2 in [VI]. We have replaced the original tidal model ME01 with model ME02. Gravity residuals and regression coefficients for different methods of correcting SG data for atmospheric and Baltic loading from 1st December 1994 to 31st August 2002, GR = gravity residuals. HSL = Sea level at Helsinki TG, DSL = Sea level at Degerby TG, 310=admittance for air pressure corrections from earlier analysis ($-3.10 \text{ nms}^{-2}/\text{hPa}$). HRL=air pressure corrected with HIRLAM, AP = local air pressure and regression.

Treatment	Loading of Baltic Sea		Error (nms^{-2})	Correlation coefficient	STD gravity Residual (nms^{-2})	Reduction percent
	Air pressure coefficient ($\text{nms}^{-2}/\text{hPa}^{-1}$)	Regression coefficient ($\text{nms}^{-2}/\text{m}^{-1}$)				
GR					39.08	
GR 310	-3.10				10.58	± 0
GR 310 / HSL	-3.10	20.74	0.16	0.464	9.37	-11
GR 310 / DSL	-3.10	22.55	0.18	0.448	9.46	-11
GR AP	-3.16				10.56	± 0
GR AP /HSL	-2.91	25.44	0.18		9.16	-13
GR AP /DSL	-2.93	27.16	0.20		9.29	-12
GR HRL	HIRLAM				10.96	+3
GR HRL / HSL	HIRLAM	26.93	0.15	0.582	8.91	-16
GR HRL / DSL	HIRLAM	29.10	0.17	0.558	9.09	-14

6. Hydrological effects on gravity

6.1. Instrumentation and available data

At a distance of 3 m from the T020 there is a 33 m deep borehole in the bedrock, with a diameter of 11 cm, for monitoring the groundwater (GW). The level was measured manually since November 1994. In March 1998 a pressure sensor for the level measurements was installed in the borehole and connected to the DAS. In addition, we have used another access tube for monitoring groundwater moisture on a swamp at 80 m distance from October 1999 to October 2001. This tube was also equipped with pressure sensor and connected to the DAS.

A tipping buckets rain gauge (CASELLA 100000E) was installed in an open area near the laboratory in May 1999. The range of local annual precipitation is 450 mm to 810 mm (1995 – 2004). This instrument cannot measure snowfall. The water equivalent of snow cover is measured manually with a special snow balance. The maximum varied from 50 mm to 80 mm (1994 – 2004). For lacking precipitation and snow data, we have exploited data available from the Finnish Meteorological Institute (Ilmastokatsaus, 1994-2005) and from the Finnish Environment Institute (MHR, 1994 – 2005). Local weather data outside of the laboratory (air pressure, temperature and humidity) are available since June 1997. Fluctuation of air temperature at ME is from -30° to $+30^{\circ}$. In addition, since June 1998 wind and solar radiation data are available.

For modeling local hydrological effects a terrain model was constructed. Heights were measured for more than 2100 points up to a distance 100 – 150 m with tacheometer, in years 1999 - 2000. The digital height map of the National Land Survey of Finland was

used (25 m grid) beyond this area. The detection threshold of transient gravity changes for SG is about a nms^{-2} corresponding 2 mm water as Bouguer approximation. The calculated gravity effect of a 10 mm water layer on the surface for area 200×200 m around the SG is 1.2 nms^{-2} excluding the building area. For a larger area 1×1 km we get only a 0.2 nms^{-2} more. The calculated total effect is thus 1/3 of the Bouguer plate approximation. We should expect detectable effects (about 3 nms^{-2}) in gravity for a sudden shower of 10 mm and $7\text{-}11 \text{ nms}^{-2}$ maximally for the snow cover.

To estimate soil moisture effects, the thickness of soil above bedrock was determined with gravimetric techniques and by drilling up to a distance 100 m. The mean soil thickness around the laboratory is 0.75 m and the maximum 3.8 m. Calculations show that a change by 10 % in the moisture content of the soil (mossy moraine) changes gravity by 8 nms^{-2} .

6.2. Results of local studies

The Papers [III and IV] present results of hydrological studies with T020 at ME. The Paper [III] presents first results of clear correlation between SG gravity and groundwater level for years 1994 - 1999. This effect was found earlier with relative gravimeter by Mäkinen and Tattari (1990, 1991) and with SG by Peter et al. (1995). In the Paper [IV] we confirmed the effect of GW on the gravity from December 1994 to August 2000. We got an admittance for GW, $27 \text{ nms}^{-2}\text{m}^{-1}$ that is still usable. The RMS of gravity residuals reduced from 21 nms^{-2} to 14 nms^{-2} . Using a simple Bouguer-plate approximation, we get a specific yield of 7 %, which is high compared with the porosity of monolithic granite (1-2 %). Obviously, the water is contained in the fractures of rock. It is likely that the level in the well also acts as an indicator for the water in the sediments.

An important discovery was the effect of snow cover on the roof of the laboratory. It was found experimentally by chance. A heavy load of snow (23000 kg) was dropped from the roof. The change in gravity was $+23 \text{ nms}^{-2}$. Fortunately we had measured the properties of snow load some days before. Modeling calculations confirmed the observed results. Our recommendations for SG stations were: monitoring groundwater level, measurements of water equivalent of snow at least up to a distance of 50 m, terrain modeling and rain gauge.

For detailed investigations an additional access tube was used to monitor groundwater in the soil. The water level correlates with the level in the borehole. We have observed that heavy local precipitation has an immediate influence on gravity through surface soil moisture. Its impact on groundwater in the borehole is smoother and delayed by some hours (Fig. 4, [IV] and Hokkanen et al. (2004, 2005)). Some observations suggest that a sudden 20 mm precipitation increases temporarily gravity by about 10 nms^{-2} or more compared to the surface area model mentioned in Section 6.1. Presumably, a neighbouring area acts as a temporary reservoir. Local hydrology includes still open questions and is an object of recent studies.

We usually correct the effect of groundwater at the preprocessing stage together with the drift correction. Similar values for GW admittance are formed in tidal analyses ($27\text{-}28 \text{ nms}^{-2}\text{m}^{-1}$). The GW level 1994 - 2004 is shown in Fig. 6.1. Its range is 2.3 meters and the minimum level is about 8 meters below the SG. In Fig 6.1 we have removed from gravity data tides, pole tide and effect of air pressure ($-3.10 \text{ nms}^{-2}\text{hPa}^{-1}$). A fit between gravity residuals and GW gives $27.4 \text{ nms}^{-2}\text{m}^{-1}$ with correlation coefficient 0.79 (Fig. 6.1).

6.3. Regional and global hydrology

The papers [III, IV] treat only the local hydrology and the Newtonian attraction due to it. We have recently extended these studies to include regional and global water storage and its loading effect i.e. both the vertical deformation and the Newtonian attraction. We used two hydrological models: The Climate Prediction Center global soil moisture data set (Fan et al., 2004) and the Watershed Simulation and Forecasting System (WSFS) of the Finnish Environment Institute (Vehviläinen, et al., 2002). We have compared (Virtanen et al. 2005a; 2005b) the time series of T020 with both, using regression methods and loading calculations. A key question is the separation of the attraction of near-field water storage from the loading effect of the regional water storage, as the two are strongly correlated. A likely outcome of the study is revision of the admittance of the local groundwater level into gravity at ME (previous section).

Hydrological phenomena appear to be a main cause for the regional gravity variation detected by the gravity satellites CHAMP and GRACE. In several studies (Crossley and Hinderer, 2002; Crossley et al., 2005; Neumeyer et al. 2004; 2006; Virtanen et al. 2005a; 2005b) a correlation between regional gravity variation detected by the satellites and point gravity variation detected by the SGs has been pointed out. The question is again, which part of the SG response is driven by the regional hydrological loading and which part by the local hydrological attraction. A more detailed discussion is outside the scope of this study.

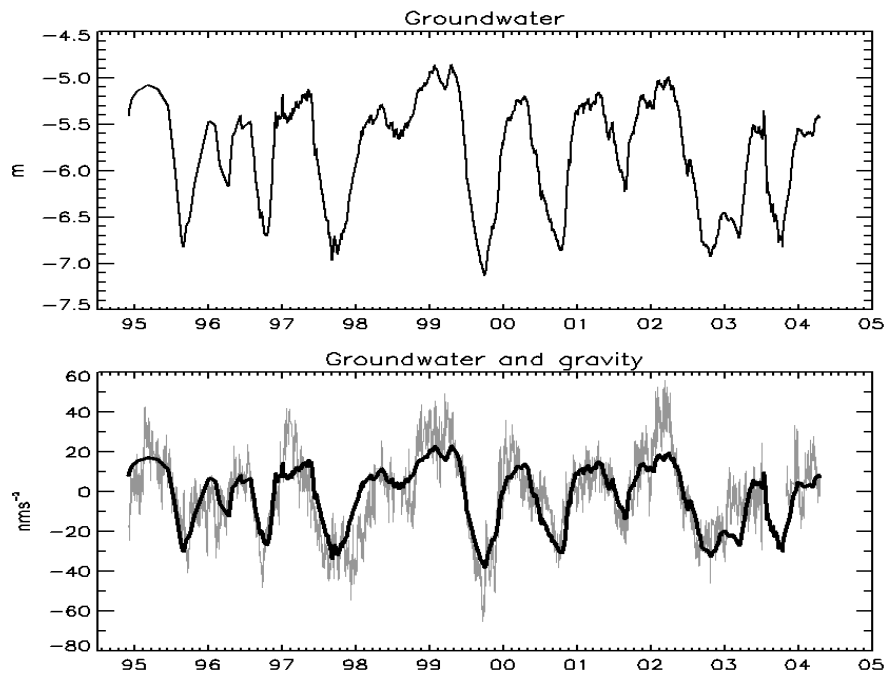


Fig. 6.1. Gravity and groundwater level at Metsähovi 1.12.1994 – 17.4.2004. Top: Groundwater level below surface, with the range of 2 meters. Bottom: Gravity residual and fitted groundwater level, the regression coefficient is $27.4 \text{ nms}^{-2}\text{m}^{-1}$ with correlation coefficient 0.79.

7. Summary and conclusions

Results of studies of Earth dynamics with the superconducting gravimeter T020 were presented from 1994 to 2005. The new data acquisition system developed by the author was described in detail. The new system has been proved to be reliable and flexible. Significantly, the accuracy of data and timing system are sufficient for SG. The health of the whole installation of T020 can be detected via an Internet connection.

Metsähovi belongs to the group of low noise SG stations and is thus suitable for studies in seismic frequency band. Information on the nature of microseism at Metsähovi was presented. Annual variations, spectral distributions, amplitudes and sources were given. There is a clear correlation between the occurrence of a low atmospheric pressure (storm) in the Northern Atlantic Ocean and microseism.

Free oscillation phenomena of the Earth excited by great earthquakes were investigated. Spectra, studies of attenuation and rotational splitting were presented. All the lowest modes of different oscillation types are found (${}_0S_2$, ${}_0T_2$ and ${}_0S_0$). The strongest earthquake (Mw 9.0) ever observed with T020 happened in Sumatra on December 26, 2004. The amplitude of ground motion due to mode ${}_0S_0$ was a few days after quake about 0.05 mm, exceeding 10 times that of a strong microseism. This mode was clearly detectable still 3 months after the earthquake. A special phenomenon is incessant excitation of the Earth's free oscillation. The amplitude is on the order of 1 ngal. The detection of this oscillation with T020 was shown from August 1994 to August 1998.

With the T020 the precise local tidal parameters were determined. The importance of accuracy of local tidal model used in the data analyses was demonstrated. Hydrological effects on gravity such as variation in groundwater level, precipitation, soil moisture and snow cover were studied. The variation in the local groundwater level correlates significantly (0.79) with gravity. The range was about 2 m and the regression coefficient $27 \text{ nms}^{-2}\text{m}^{-1}$. This phenomenon was taken into account in an early stage in the data processing. One important finding was that the local snow cover affects notably on gravity.

We have computed the effects of the variation in atmospheric mass, and of the loading by the Baltic Sea in gravity. Examinations utilize both regression methods based on a single tide gauge/barometer, and calculations with detailed models for the surface loads. Theoretical loading calculations using Green's functions formalism were performed for both vertical motion and gravity. A uniform layer of water covering the complete Baltic Sea increases the gravity at Metsähovi by $31 \text{ nms}^{-2}\text{m}^{-1}$ and the vertical deformation is -11 mm. Regressing the gravity residual for 1994 – 2002 on the nearest tide gauge at Helsinki gave the coefficient $26.9 \text{ nms}^{-2}\text{m}^{-1}$, which is 87% of the model value for a uniform layer of water. Loading studies were associated with temporal height variations using the GPS data of Metsähovi permanent station. Loading by air pressure and the Baltic Sea explains about 40% of the variance of daily GPS height solution.

Results of long time series at Metsähovi demonstrated high quality of data and correctly carried out offsets and drift corrections. The superconducting gravimeter T020 has been proved to be an eminent and versatile tool in studies of the Earth dynamics.

References

- Arabelos, D., 2002. Comparison of Earth-tide parameters over a large latitude difference. *Geophys. J. Int.* 151, 950-956.
- Baker, T. and Bos, M., 2001. Tidal Gravity Observations and Ocean Tide Models. *J. Geod. Soc. Japan* 47 (1), 76-81.
- Baker, T. and Bos, M., 2003. Validating Earth and ocean tide models using tidal gravity measurements. *Geophys. J. Int.* 152, 468-485.
- Banka, D., 1997. Noise levels of superconducting gravimeters at seismic frequencies, PhD thesis, GDMB-Informationgesellschaft mbH, Clausthal, Germany.
- Banka, D. and Crossley, D.J., 1999. Noise levels of superconducting gravimeters at seismic frequencies, *Geophys. J. Int.* 139, 87-97.
- Boy, J.-P., M. Llubes, J. Hinderer, and N. Florsch, 2003. A comparison of tidal ocean loading models using superconducting gravimeter data. *J. Geophys. Res.* 108 (B4), 2193, doi: 10.1029/2002JB002050.
- Crossley, D., Hinderer, J., Casula, G., Francis, O., Hsu, H.-T., Imanishi, Y., Jentzsch, G., Kääriäinen, J., Merriam, J., Meurers, B., Neumeyer, J., Richter, B., Shibuya, K., Sato, T. and van Dam, T., 1999. Network of superconducting gravimeters benefits a number of disciplines. *Trans. Am. Geophys. U.* 80, 121-126.
- Crossley, D., and Hinderer, J., 2002. GGP Ground Truth for Satellite Gravity Missions. *Bull. d'Inf. Marées Terr.* 136, 10735-10742.
- Crossley, D., Hinderer, J., Boy, J.-P., 2004. Regional gravity variations in Europe from superconducting gravimeters. *J. Geodyn.* 38 (3-5), 325-342.
- Crossley, D., Hinderer, J., Boy, J.-P., 2005. Time variations of the European gravity field from superconducting gravimeter. *Geophys. J. Int.*, 161, 257-264.
- Dehant, V., Defraigne, P., Wahr, J., 1999. Tides for a convective Earth. *J. Geophys. Res.* 104 (B1), 1035-1058.
- Ducarme, B., Vandercoilden, L., 2000. First Results of the GGP data Bank At ICET, *Cahiers du Centre Européen de Géodynamique et de Séismologie* 17, 117-124.
- Ducarme, B. and Sun, H.-P., 2001. Tidal gravity results from GGP network in connection with tidal loading and Earth response, *J. Geod. Soc. Jap.* 47 (1), 308-315.
- Ducarme, B., Sun, H.-P., Xu, J.-Q., 2002. New investigations of tidal gravity results from the GGP network, *Bull. d'Inf. Marées Terr.* 136, 10761-10766.
- Ducarme, B., Venedikov, A., Arnoso, J., Vieira, R., 2004. Determination of the long period tidal waves in the GGP superconducting gravity data. *J. Geodyn.* 38 (3-5), 307-324.
- Dunn, B., 1994. CSGI Software Reference Manual, Revision 3.1. Dept. Earth Sciences, The University of Western Ontario, London, Ontario, Canada.
- Fan, Y., Van den Dool, H., 2004. The CPC global monthly soil moisture data set at 1/2 degree resolution for 1948-present. *J. Geophys. Res.* 109, D10102, doi: 10.1029/2003JD004345.
- GGP, 2003. CD-ROM ETGGP #5A, The GGP consortium. <http://ggp.gfz-potsdam.de/>.
- GGP, 2006. GGP Home Page. <http://www.eas.slu.edu/GGP/ggphome.html>.
- Goodkind, J., 1999. The superconducting gravimeter, *Review of Scientific Instruments* 70 (11), 4131-4152.
- GWR, 1989. Superconducting gravity meter, Operational Manual, Serie #019, San Diego, USA.

- Hinderer, J., Amalvict, M., Francis, O. and Mäkinen, J., 1998. On the calibration of superconducting gravimeters with the help of absolute gravity measurements, in: Proc. 13th Int. Symp. Earth Tides, Brussels 1997, 557-564, Observatoire Royal de Belgique.
- Hinderer, J., Crossley, D., 2000. Time variations in gravity and inferences on the Earth's structure and dynamics. *Surveys in Geophysics* 21, 1–45.
- Hinderer, J., Crossley, D., 2004. Scientific achievements from the first phase (1997-2003) of the Global Geodynamics Project using a worldwide network of superconducting gravimeters. *J. Geodyn.* 38 (3-5), 237-262.
- Hokkanen, T., Virtanen, H., Pirttivaara, M., 2004. Groundwater, soil moisture, and superconducting gravimeter data. European Association of Geoscientists and Engineers (EAGE), 66th Conference and Exhibition, Paris, 7–10 June, 2004. Abstract and poster.
- Hokkanen, T., Virtanen, H., Pirttivaara, M., 2005. On the hydrogeological noise in superconducting gravimeter data. Submitted to *Near Surface Geophysics*.
- Ilmastokatsaus, 1994–2005. Finnish Meteorological Institute, (Monthly survey in Finnish).
- Jentsch, G., Crossley, D., Hinderer, J., Takemoto, S., 2004. Time varying gravimetry, GGP and vertical motions *J. Geodyn.* 38 (3-5).
- MHR, 1994-2005. Monthly Hydrological Report, Finnish Environment Institute, Hydrology and Water Management Division, 1994 – 2005, Helsinki.
- Mäkinen, J., Tattari, S., 1990. The influence of variation in subsurface water storage on observed gravity, Proc. 11th Int. Symp. Earth Tides, ed. J. Kakkuri, Schweitzerbart. Verlag, Stuttgart, 457-471.
- Mäkinen, J., Tattari, S., 1991. Subsurface water and gravity, in Proceedings of the Workshop: Non Tidal Gravity Changes Intercomparison between absolute and superconducting gravimeters. Ed. Poitevin, C., Cahiers du Centre Européen de Géodynamique et de Séismologie 3, 235-240.
- Mäkinen, J., Kääriäinen, J., Virtanen, H., 1995. Calibration of a superconducting gravimeter using short sets of simultaneous observations with an absolute gravimeter. Poster presented at XXI General Assembly of IUGG in Boulder, USA.
- Nawa, K., Suda, N., Fukao, Y., Sato, T., Aoyama, Y., Shibuya, K., 1998. Incessant excitation of the Earth's free oscillations, *Earth, Planets and Space*, 50 (1), 3-8.
- Nawa, K., Suda, N., Fukao, Y., Sato, T., Tamura, Y., Shibuya, K., McQueen, H., Virtanen, H., Kääriäinen, J., 2000. Incessant excitation of the Earth's free oscillations: global comparison of superconducting gravimeter records, *Phys. Earth planet. Int.* 120, 289-297.
- NEIC, 2005. National Earthquake Information Center. USGS Earthquake Hazards Program web site: <http://www.earthquake.usgs.gov/>.
- Neumeyer, J., Schwintzer, P., Barthelmes, F., Dierks, O., Imanishi, Y., Kroner, C., Meurers, B., Sun, H.-P., Virtanen, H., 2004. Comparison of Superconducting Gravimeter and CHAMP Satellite Derived Temporal Gravity Variations. Ed. C. Reigber et al. *Earth Observations with Champ, Results from Three Years in Orbit*. Springer, 31-36.
- Neumeyer, J., Barthelmes, F., Dierks, O., Flechtner, F., Harnisch, M., Harnisch, G., Hinderer, J., Imanishi, Y., Kroner, C., Meurers, B., Petrovic, S., Reigber, Ch., Schmidt, R., Schwintzer, P., Sun, H.-P., Virtanen, H., 2006. Combination of temporal gravity variations resulting from Superconducting Gravimeter recordings, GRACE satellite observations and global hydrology models. *J. Geodesy*, doi: 10.1007/S00190-005-0014-8.
- Peter, G., Klopping, F.J., Berstis, K.J., 1995. Observing and Modeling Gravity Changes Caused by Soil Moisture and Groundwater Table Variations with Superconducting Gravimeters in Richmond, Florida, U.S.A, Cahiers du Centre Européen de Géodynamique et de Séismologie 11, 147-158.

- Peterson, J., 1993. Observations and modelling of seismic background noise. Open-File report 93-332, U.S. Department of Interior, Geological Survey, Albuquerque, New Mexico.
- Prothero, W.A., Goodkind, J., 1968. A superconducting gravimeter. *Rev. Sci. Instr.* 39 (9), 1257–1268.
- Rosat, S., Hinderer, J. and D. Crossley, 2002. A comparison of the seismic noise levels at various GGP stations, *Bull. d'Inf. Marées Terr.* 135, 10689-10700.
- Rosat, S., Hinderer, J., Crossley, D., and J. P. Boy, 2004. Performance of superconducting gravimeters from long period seismology to tides. *J. Geodyn.* 38 (3-5), 461-476.
- Scherneck, H.-G., 1994. Realistic modelling of deformations due to air pressure variations. In: Harsson, B.G., Ness, J.A., (Eds.), *Proceedings of the 12th General Meeting of the Nordic Geodetic Commission*, Ullensvang, Norway, 30 May – 3 June 1994, 229-243.
- Smylie, D., Francis, O., Merriam, J., 2001. Beyond tides-determinations of core properties from superconducting gravimeter observations. *J. Geodet. Soc. Japan* 47 (1), 364-372.
- Sun, H.-P., Hsu, H.-T., Jentzsch, G., and Xu, J.-Q., 2002a. Tidal gravity observations obtained with a superconducting gravimeter at Wuhan/China and its application to geodynamics, *J. Geodyn.* 33 (1-2), 187-198.
- Sun, H.-P., Xu, J-Q, and Ducarme, B., 2002b. Preliminary results of the Free Core Nutation eigenperiod obtained by stacking SG observations at GGP stations, *Bull. d'Inf. Marées Terr.* 136, 10725-10728.
- Van Camp, M., Wenzel, H.-G., Schott, P., Vauterin, P. and Francis, O., 2000. Accurate transfer function determination for superconducting gravimeters. *Geophys. Res. Let.* 27 (1), 37-40.
- Van Camp, M., and Vauterin, P., 2005. Tsoft: graphical and interactive software for the analysis of time series and Earth tides, *Computers & Geosciences* 31 (5), 631-640.
- Van Dam, T.M. and Wahr, J., 1998. Modeling environment loading effects: a Review. *Phys. Chem. Earth* 23 (9–10), 1077–1087.
- Vehviläinen, B. and Huttunen, M., 2002. The Finnish watershed simulation and forecasting system (WSFS). XXI Conference of the Danubian countries on the hydrological forecasting and hydrological bases of water management. Bucharest, Romania. 2-6 September 2002.
- Virtanen, H., Kääriäinen, J., 1995. The installation of and first results from the superconducting gravimeter GWR20 at the Metsähovi station, Finland. *Rep. Finn. Geod. Inst.* 95:1, 1–15.
- Virtanen, H., Kääriäinen, J., 1997. The GWR T020 superconducting gravimeter 1994–1996 at the Metsähovi station, Finland. *Rep. Finn. Geod. Inst.* 97:4, 1–26.
- Virtanen, H., Mäkinen, J., 2003: Air pressure and Baltic Sea loading corrections to gravity data at Metsähovi. In: Poutanen, M. Suurmäki, H. (Eds), *Proceedings of the XIV General Meeting of the Nordic Geodetic Commission*. 148-153.
- Virtanen, H., Bilker, M., Mäkinen, J., Poutanen, M, Tervo, M., Vehviläinen, B., Huttunen, M., Mäkinen, R., 2005a. Comparison of modeled variation in water storage in Finland with GRACE and superconducting gravimeter observations. *Geophysical Research Abstracts* 7, 06248, 2005.
- Virtanen, H., Bilker, M., Mäkinen, J., Tervo, M., Vehviläinen, B., Huttunen, M, Mäkinen, R., Peltoniemi, M., Hokkanen, T., Pirttivaara, M., 2005b. Comparison of modelled variation in water storage in Finland with superconducting gravimeter observations and with GRACE. Abstract in *Dynamic Planet*, Cairns, Australia, 22-26 August 2005.
- Warburton, R. J. and Brinton, E.W., 1995. Recent developments in GWR Instruments' superconducting gravimeters, in *Proceedings of Second Workshop: Non-tidal gravity changes Intercomparison between absolute and superconducting gravimeters*, 11, 23-56, *Cahiers du Centre Européen de Géodynamique et de Séismologie* 11, 23-56.

- Wenzel H.-G. ,1996. The nanogal software: earth tide data processing package ETERNA 3.30, Bull. d'Inf. Marées Terr. 124, 9425-9439.
- Widmer-Schmidrig, R., 2003. What Can Superconducting Gravimeters Contribute to Normal –Mode Seismology. Bulletin of the Seismological Society of America 93 (3), 1370-1380.
- Xu, J., Sun, H., Ducarme, B., 2004. A global experimental model for gravity tides of the Earth. Journal of Geodynamics 38 (3-5), 293-306.
- Zürn, W., Laske, G., Widmer-Schmidrig, R., and Gilbert, F., 2000. Observations of Coriolis coupled modes below 1 mHz., Geophys. J. Int. 143, 113-118.

Appendices

Appendix 1

Local tidal model ME01 used in Papers [III-VI]. The format is same as used in the database for TSOFT program to calculate theoretical tide. The values for SA and SSA are a priori values. Other factors are based on the analysis (Section 4.1).

Columns are: COMP:, from [cpd], to [cpd], amplitude factor, phase (degree), Wave name.

```
[TIDECOMP] Metsahovi
NAME: ME01
TYPE: 1
AZIM: 0.0000000
GRAV: 0.0000000
COMP: 0.001379 0.004107 1.16000 0.0000 SA
COMP: 0.004108 0.020884 1.16000 0.0000 SSA
COMP: 0.020885 0.054747 1.14061 1.1762 MM
COMP: 0.054748 0.091348 1.15033 -0.1140 MF
COMP: 0.091349 0.501369 1.10530 1.2223 MTM
COMP: 0.721499 0.851182 1.14121 -3.7435 138
COMP: 0.852095 0.857261 1.12703 -1.0110 2Q1
COMP: 0.857571 0.870022 1.15817 -0.6001 SIG1
COMP: 0.887327 0.894010 1.14475 0.0216 Q1
COMP: 0.895216 0.906314 1.14996 -0.0243 RO1
COMP: 0.921941 0.932582 1.15364 0.2635 O1
COMP: 0.932583 0.940487 1.14979 0.3569 TAU1
COMP: 0.958085 0.968565 1.16256 0.0052 M1
COMP: 0.968565 0.974188 1.15184 0.6248 CHI1
COMP: 0.989048 0.994755 1.14928 0.3137 PI1
COMP: 0.995143 0.998028 1.15501 0.0503 P1
COMP: 0.999852 1.000147 1.08534 6.9280 S1
COMP: 1.001824 1.003651 1.14099 0.0902 K1
COMP: 1.005328 1.005622 1.24159 1.1047 PSI1
COMP: 1.007594 1.011098 1.18278 -0.4384 FI1
COMP: 1.013689 1.034319 1.16873 -0.8384 THE1
COMP: 1.034466 1.044799 1.15238 0.0780 J1
COMP: 1.064841 1.073202 1.17702 0.1981 SO1
COMP: 1.073349 1.080797 1.15405 0.1773 OO1
COMP: 1.080944 1.216396 1.17691 1.3099 V1
COMP: 1.719380 1.827342 1.10910 2.6648 3N2
COMP: 1.827799 1.853920 1.16178 1.4845 EPS2
COMP: 1.854524 1.863634 1.18042 1.4072 2N2
COMP: 1.864090 1.872141 1.16975 0.9096 MI2
COMP: 1.888387 1.900529 1.18165 1.1068 N2
COMP: 1.900544 1.906461 1.18177 1.0229 NI2
COMP: 1.923765 1.942753 1.18219 0.7123 M2
COMP: 1.958232 1.966446 1.16507 0.6909 LMB2
COMP: 1.966446 1.976926 1.17381 0.3273 L2
COMP: 1.991786 1.998287 1.18112 -0.1277 T2
COMP: 1.999705 2.000766 1.17619 0.0376 S2
COMP: 2.002590 2.002885 1.17666 1.9503 R2
COMP: 2.003032 2.031287 1.17797 0.1372 K2
COMP: 2.031434 2.044652 1.16843 0.6820 ETA2
COMP: 2.047243 2.182843 1.16785 -6.8226 2K2
COMP: 2.753243 2.869713 1.07639 0.5531 493
COMP: 2.892640 2.935615 1.08064 0.1416 M3
COMP: 2.940177 3.081253 1.05915 -2.9201 SO3
COMP: 3.791963 3.937896 1.04195 -155.9466 M4
```


Appendix 2

Tidal model ME02 by the author (Section 4.1). The air pressure was corrected by HIRLAM. Sea level at Helsinki (HSL) is given as a hydrological regression parameter. Picked from ETERNA output file (*.prm).

```

Program ANALYZE, version 3.40 970921                File: 9402icet
#####
# STATION 0892 METSÄHOVI                          Tidal gravity #
# SUPERCONDUCTING GRAVIMETER T020                 #
#                                                  #
#TIME LAG : 0.0690 DEG/CPD 19941201-19970905      #
#TIME LAG : 0.0395 DEG/CPD 19970905-19990315      #
#TIME LAG : 0.0690 DEG/CPD 19990315-20010103      #
#TIME LAG : 0.0395 DEG/CPD 20010103-20020901      #
#                                                  #
#####
Latitude: 60.2172 deg, longitude: 24.3958 deg, azimuth: 0.0000 deg.
19941201...20020901      6 blocks. Recorded days in total: 2620.250
Tamura (1987)           TGP, threshold: 0.100E-06      1200 waves.
WAHR-DEHANT-ZSCHAU inelastic Earth model used.
UNITY window used for least squares adjustment.
Sampling interval:      3600. s
Numerical filter is no filter      with      1 coefficients.

Average noise level at frequency bands in nm/s**2
0.1 cpd  0.205255      1.0 cpd  0.037358      2.0 cpd  0.015280
3.0 cpd  0.008175      4.0 cpd  0.005918      white noise 0.060376

adjusted tidal parameters :

              theor.
from         to         wave  ampl. ampl.fac.  stdv. ph. lead  stdv.
[cpd]       [cpd]       [nm/s**2 ] [deg] [deg] [deg]
0.001379 0.004107 SA      5.9754  1.10663  1.32758  2.9714  60.1225
0.004108 0.006666 SSA     37.6292  1.23145  0.07980  -2.4142  3.7706
0.006667 0.020884 STA     2.1970  1.67455  0.92567  -20.4141 31.3226
0.020885 0.054747 MM      42.7154  1.14292  0.00949  0.0999  0.4748
0.054748 0.091348 MF      80.8658  1.15111  0.00342  0.2359  0.1700
0.091349 0.501369 MTM    15.4827  1.15120  0.01152  -0.0601  0.5733
0.721499 0.833113 SGQ1   1.9800  1.15848  0.01513  -0.2929  0.7480
0.851182 0.859691 2Q1    6.7910  1.13973  0.00477  -0.5801  0.2396
0.860896 0.870023 SGM1   8.1960  1.14641  0.00404  -0.1872  0.2021
0.887325 0.896130 Q1    51.3220  1.14868  0.00064  0.0862  0.0319
0.897806 0.906315 RO1    9.7484  1.15284  0.00340  -0.2994  0.1691
0.921941 0.930449 O1    268.0524  1.15488  0.00012  0.2400  0.0061
0.931964 0.940488 TAU1   3.4961  1.14117  0.00736  -0.5997  0.3697
0.958085 0.966756 NO1   21.0813  1.15848  0.00140  0.1225  0.0691
0.968565 0.974189 CHI1   4.0319  1.14688  0.00817  0.2929  0.4083
0.989048 0.995144 PI1    7.2941  1.16307  0.00409  0.0333  0.2015
0.996967 0.998028 P1   124.7242  1.15546  0.00024  0.0704  0.0119
0.999852 1.000148 S1     2.9495  1.21576  0.01425  4.4714  0.6717
1.001824 1.003651 K1    376.9855  1.14158  0.00009  0.0563  0.0043
1.005328 1.005623 PSI1   2.9494  1.28043  0.01017  -0.8495  0.4551
1.007594 1.013689 PHI1   5.3682  1.16740  0.00553  -0.3242  0.2712
1.028549 1.034467 TET1   4.0311  1.17056  0.00812  0.9550  0.3973
1.036291 1.044800 J1    21.0805  1.16049  0.00150  0.0439  0.0739
1.064841 1.071083 SO1    3.4969  1.16366  0.00972  0.4978  0.4787
1.072583 1.080945 OO1   11.5349  1.15710  0.00347  0.0337  0.1718
1.099161 1.216397 NU1    2.2085  1.16382  0.01681  0.1935  0.8273
1.719380 1.837970 EPS2   1.3704  1.15143  0.00773  0.9883  0.3848
1.853920 1.862429 2N2    4.6999  1.17172  0.00242  1.2175  0.1185
1.863634 1.872142 MU2    5.6720  1.17017  0.00209  0.9669  0.1026
1.888387 1.896748 N2    35.5178  1.17800  0.00033  1.0161  0.0160
1.897954 1.906462 NU2    6.7463  1.17909  0.00176  1.0614  0.0857
1.923765 1.942754 M2   185.5103  1.18086  0.00006  0.7016  0.0031
1.958232 1.963709 LAM2   1.3680  1.17003  0.00867  0.7425  0.4247
1.965827 1.976926 L2    5.2435  1.17535  0.00209  0.3682  0.1019
1.991786 1.998288 T2    5.0462  1.17061  0.00243  0.2169  0.1191
1.999705 2.000766 S2    86.3092  1.17595  0.00014  0.0564  0.0069
2.002590 2.013689 K2    23.4632  1.17708  0.00061  0.2069  0.0297
2.031287 2.047390 ETA2   1.3119  1.17159  0.01046  0.1085  0.5115
2.067579 2.182844 2K2    0.3436  1.19443  0.03986  -2.1171  1.9117
2.753243 2.869714 MN3    0.4974  1.07849  0.01197  0.6226  0.6358
2.892640 3.081254 M3    1.8128  1.08375  0.00345  0.2880  0.1824
3.791963 3.901458 M4    0.0164  0.15380  0.25793  167.6555 96.0933

```

Adjusted meteorological or hydrological parameters:

no.	regr.coeff.	stdv.	parameter	unit
1	27.11662	0.15877	HSL	nm/s**2 / m
2	1.13512	0.29448	pole tide	nm/s**2 /nm/s**2
3	6.14657	18.61204	dpoltid/dt	nm/s**2 /nm/s**2/d

Correlation matrix of meteorological regression parameters:

	HSL	pole tide	dpoltid/dt
HSL	1.000	-0.016	-0.100
pole tide	-0.016	1.000	0.020
dpoltid/dt	-0.100	0.020	1.000

Adjusted TSCHEBYSCHIEFF polynomial bias parameters :

block	degree	bias	stdv.
1	0	22.360108 nm/s**2	0.080237 nm/s**2
2	0	36.686186 nm/s**2	0.154047 nm/s**2
3	0	10.675285 nm/s**2	0.078319 nm/s**2
4	0	17.861077 nm/s**2	0.128412 nm/s**2
5	0	17.530137 nm/s**2	0.095762 nm/s**2
6	0	15.186247 nm/s**2	0.077397 nm/s**2

Standard deviation:	8.542 nm/s**2
Degree of freedom:	62793
Maximum residual:	39.367 nm/s**2
Maximum correlation:	0.519 dpoltid/dt with X-wave-SA
Condition number of normal equ.	10.642

Appendix 3

Results of analyses for diurnal and shorter waves by the author (ME03). Air pressure used as a meteorological regression parameter. Picked from ETERNA out file (*.prn).

```

Program ANALYZE, version 3.40 970921          File: 9402icet
#####
# STATION 0892 METSÄHOVI                    Tidal gravity #
# SUPERCONDUCTING GRAVIMETER T020          #
#                                           #
#TIME LAG : 0.0690 DEG/CPD 19941201-19970905 #
#TIME LAG : 0.0395 DEG/CPD 19970905-19990315 #
#TIME LAG : 0.0690 DEG/CPD 19990315-20010103 #
#TIME LAG : 0.0395 DEG/CPD 20010103-20020901 #
#                                           #
#####
Latitude: 60.2172 deg, longitude: 24.3958 deg, azimuth: 0.0000 deg.
19941201...20020901      6 blocks. Recorded days in total: 2620.250
Tamura (1987)           TGP, threshold: 0.100E-06      1200 waves.
WAHR-DEHANT-ZSCHAU inelastic Earth model used.
UNITY window used for least squares adjustment.
Sampling interval:      3600. s
Numerical filter is PERTZEV59 with 51 coefficients.

Average noise level at frequency bands in nm/s**2
0.1 cpd*****          1.0 cpd  0.031835      2.0 cpd  0.013862
3.0 cpd  0.007950      4.0 cpd  0.005573      white noise 0.006880

adjusted tidal parameters :

      theor.
from   to   wave  ampl. ampl.fac.  stdv. ph. lead  stdv.
[cpd] [cpd] [nm/s**2] [nm/s**2] [deg] [deg]
0.721499 0.833113 SGQ1  1.9800  1.15529  0.01448 -1.0346  0.7182
0.851182 0.859691 2Q1  6.7910  1.14060  0.00435 -0.7903  0.2188
0.860896 0.870023 SGM1  8.1960  1.15173  0.00368 -0.1611  0.1829
0.887325 0.896130 Q1   51.3220  1.14709  0.00056  0.0057  0.0282
0.897806 0.906315 RO1  9.7484  1.14675  0.00299 -0.1132  0.1493
0.921941 0.930449 O1   268.0524  1.15321  0.00011  0.2618  0.0053
0.931964 0.940488 TAU1 3.4961  1.15241  0.00632 -0.0732  0.3145
0.958085 0.966756 NO1  21.0813  1.15949  0.00119  0.2338  0.0588
0.968565 0.974189 CHI1 4.0319  1.15817  0.00696  0.1259  0.3442
0.989048 0.995144 PI1  7.2941  1.15230  0.00348  0.1807  0.1732
0.996967 0.998028 P1   124.7242  1.15425  0.00020  0.0639  0.0101
0.999852 1.000148 S1   2.9495  1.14872  0.01215  7.4811  0.6059
1.001824 1.003651 K1   376.9855  1.14055  0.00007  0.0793  0.0036
1.005328 1.005623 PSI1 2.9494  1.25785  0.00868  0.4927  0.3954
1.007594 1.013689 PHI1 5.3682  1.17185  0.00472 -0.6954  0.2308
1.028549 1.034467 TET1 4.0311  1.17252  0.00700  0.1097  0.3418
1.036291 1.044800 J1   21.0805  1.15796  0.00129  0.0400  0.0640
1.064841 1.071083 SO1  3.4969  1.16098  0.00856  0.2389  0.4228
1.072583 1.080945 OO1  11.5349  1.15432  0.00307  0.0051  0.1523
1.099161 1.216397 NU1  2.2085  1.16790  0.01539  0.2680  0.7551
1.719380 1.837970 EPS2 1.3704  1.15185  0.00747  1.0880  0.3714
1.853920 1.862429 2N2  4.6999  1.17220  0.00227  1.3521  0.1110
1.863634 1.872142 MU2  5.6720  1.16855  0.00196  1.0099  0.0959
1.888387 1.896748 N2   35.5178  1.17864  0.00030  1.0389  0.0147
1.897954 1.906462 NU2  6.7463  1.18035  0.00161  1.1019  0.0782
1.923765 1.942754 M2   185.5103  1.18133  0.00006  0.7079  0.0028
1.958232 1.963709 LAM2 1.3680  1.16738  0.00782  0.5754  0.3839
1.965827 1.976926 L2   5.2435  1.17606  0.00188  0.3802  0.0918
1.991786 1.998288 T2   5.0462  1.17251  0.00221  0.1630  0.1078
1.999705 2.000766 S2   86.3092  1.17552  0.00013  0.0765  0.0063
2.002590 2.013689 K2   23.4632  1.17752  0.00055  0.1800  0.0270
2.031287 2.047390 ETA2 1.3119  1.17656  0.00968 -0.2109  0.4714
2.067579 2.182844 2K2  0.3436  1.17577  0.03790 -2.4586  1.8468
2.753243 2.869714 MN3  0.4974  1.07710  0.01190  0.6315  0.6328
2.892640 3.081254 M3   1.8128  1.08188  0.00329  0.3410  0.1744
3.791963 3.901458 M4   0.0164  0.41165  0.24206 158.6900 33.6911

Adjusted meteorological or hydrological parameters:

no. regr.coef.      stdv.  parameter  unit
1      -3.64710      0.00443  Airpress  nm/s**2 /hPa

Standard deviation:      0.971  nm/s**2
Degree of freedom:      62513
Maximum residual:      15.275  nm/s**2
Maximum correlation:    0.101  Airpress  with X-wave-S2
Condition number of normal equ. 1.539

```


Publications